Lamie, Nathan. (2020). Methods to Enhance Mechanical Recovery in Arctic Conditions. (Bureau of Safety and Environmental Enforcement Oil Spill Response Research Project # 1082).

Bureau of Safety and Environmental Enforcement (BSEE) Report: Methods to Enhance Mechanical Recovery in Arctic Conditions

Nathan Lamie, Leonard Zabilansky PE, Alex Stott, Kemal Arsava, and Brandon Booker

U.S Army Engineering Research and Development Center's Cold Regions Research and Engineering Laboratory

US Department of the Interior
Bureau of Safety and Environmental Enforcement

Bureau of Safety and Environmental Enforcement

EXECUTIVE SUMMARY

This project focused on improving oil spill recovery methods in Arctic conditions by developing and accessing techniques to (1) herd oil under an ice sheet, (2) increase recovery efficiencies of a VAB skimmer, and (3) increase the pumping efficiency of an oil/water mixture in sub-freezing temperatures.

In Task 1 we showed that oil can be displaced and relocated from a sub-surface air pocket in an acrylic sheet using supplied air and we developed a U-shape air applicator attached to an underwater ROV for field use. We showed that the ROV and air applicator system successfully dislodge and relocated oil trapped under an ice sheet in a field test; however, we were not able to get the oil and air to move to a predetermined recovery location. We also found that warm supplied air may cause oil to become entrapped in the ice sheet. We recommend investigating how profiling an ice sheet to determine likely channels for passive air-oil flow prior to underwater ROV herding can influence the ability to move oil to an intend recovery location. We also recommend investigating how supplied air temperatures may influenced oil entrapment in an ice sheet.

In Task 2 we assessed the rate of ice accumulation on a VAB skimmer and showed that steam can be applied for attenuation. We developed a steam application collar as an accessory to VAB skimmers currently available on the market. We showed that while the steam collar can reduce ice accumulation on the adhesion belt it did not have a significant impact on oil recovery rates. However, it may prolong the ability of the VAB skimmer to recover oil in subfreezing temperatures. We showed that ice accumulates faster as temperature decrease; therefore, this system should be further tested in colder environments. We also recommend assessing incremental versus continuous use to reduce the amount of energy required to operate the system.

In Task 3 we showed that by applying heat to a steel pipe, we can increase the temperature of a flowing oil-water mix. We established the transferable distance of this heat through a commonly used oil recovery hose in subfreezing temperature. These data can be used to establish the frequency of this heating system required to ensure continuous heating of an oil-water mix being transferred through a hose. Pumping rates were not significantly influenced by the heating systems relative to the no-heat (control) tests. We concluded that this was due to insufficient hose length and cold temperatures to reduce pumping rates during the control tests. Therefore, future tests should include longer hoses and cooler temperatures. We also recommend investigating different oil-to-water ratios and the impact of weathering on oil pumping efficiency

REPORT AVAILABILITY

To download a PDF file of this report, go to https://www.bsee.gov/research-record/osrr-1082-methods-to-enhance-mechanical-recovery-in-arctic-conditions.

CITATION

[Lamie, N, Zabilansky, L, Stott, A. 2020. Methods to Enhance Mechanical Recovery in Arctic Conditions. Hanover, NH: US Department of the Interior, Bureau of Safety and Environmental Enforcement. BSEE 20xx-xxx. xx p.XX

PREFACE

This study was conducted for the Bureau of Safety and Environmental Enforcement through Inter Agency Agreement Number, E16PG00031. Nathan Lamie was the program manager, Kemal Arsava acted as Principal Investigators, and William Burch, Charles Schelewa, Alex Stott and Brandon Booker provided significant engineering and technician support during the study.

The Engineering Resources Branch (RV-E) of the US Army Engineer Research and Development Center, Cold Regions Research and Engineer Laboratory (ERDC-CRREL) performed the work. At the time of publication, Jared Oren was Chief, CEERD-RV-E. The Deputy Director of ERDC-CRREL was Dr. David Ringelberg, and the Director was Dr. Joseph Corriveau.

COL Ivan P. Beckman was the Commander of ERDC, and Dr. David W. Pittman was the Director.

ACKNOWLEDGEMENTS

We appreciate assistance from CRREL Department of Public Works personnel in maintaining the appropriate cold-room capabilities of the MEF during testing and in moderating room temperatures over night to help facilitate oil reaching appropriate temperatures for the testing schedule. We also thank John Hebert, Kelly Rowland and Peter Licciardi for providing technical knowledge of oil safety.

UNIT CONVERSION FACTORS

Multiply	By	To Obtain
cubic feet	0.02831685	cubic meters
cubic inches	1.6387064 E-05	cubic meters
cubic yards	0.7645549	cubic meters
degrees Fahrenheit	(F-32)/1.8	degrees Celsius
feet	0.3048	meters
foot-pounds force	1.355818	joules
gallons (US liquid)	3.785412 E-03	cubic meters
inches	0.0254	meters
knots	0.5144444	meters per second
miles (nautical)	1852	meters
miles (US statute)	1609.347	meters
miles per hour	0.44704	meters per second
pounds (force)	4.448222	newtons
pounds (force) per square foot	47.88026	pascals
pounds (force) per square inch	6.894757	kilopascals
quarts (US liquid)	9.463529 E-04	cubic meters
square feet	0.09290304	square meters
square inches	6.4516 E-04	square meters
square miles	2.589998 E+06	square meters
square yards	0.8361274	square meters
yards	0.9144	meters

Table of Contents

CHAPTER 1

1.1 BACKGROUND

Petroleum extraction and transport is projected to expand in the Arctic over the next few decades, increasing the threat of an oil spill in icy waters. In cold climates biodegradation of oil slows down significantly (Yang *et al.* 2009) and spilled crude oil can remain in cold habitats for decades. Therefore, it is critical that oil spill recovery methods are optimized for these regions to ensure that response teams recover oil efficiently and effectively. However, logistics and permitting limit the opportunities to test recovery equipment in arctic environments. Facilities with the capacity to simulate arctic conditions and sufficient space to operate recovery equipment play an important role in arctic oil spill response readiness. The ERDC-Cold Regions Research and Engineering Lab (CRREL) has unique operational capabilities to simulate extremely cold environments as well as ice cover waters. Utilizing the cold facilities at CRREL, we investigated techniques to improve oil recovery methods in subfreezing environments.

To gain insight on the challenges of oil spill response in the Arctic we collaborated with Alaska Clean Seas (ACS), and Alaskan based oil spill removal organization who has performed multiple winter training programs for oil spill recovery in cold climates. Working with ACS we identify three major limitations to current recovery methodologies for arctic oil spills: 1) methods for recovering oil trapped under an ice sheet are time consuming and ineffective, 2) adhesion belt recovery efficiencies are reduced as ice accumulates on the belt in subfreezing temperatures, and 3) viscosity of oil-water mixtures increases in subfreezing temperatures making them difficult to pump from recovery site to the transfer vessel. Herein, we developed techniques to address or mitigate these issues that are feasible to implement in arctic oil spill response scenarios.

When oil is released under an ice sheet it rises to the water-ice interface and settles in depressions in the bottom of the ice sheet (Figure 1.1). To date, the methods to recover this oil involve locating each depressions, cutting through the ice to release the oil, and recovering the oil from above or conducting an *in situ* burn. With this approach, recovering oil is labor intensive, time consuming and quickly becomes unfeasible as the size of the spill increases. Using an underwater Remotely Operated Vehicle (ROV) to inject air into these depressions may dislodge the oil and facilitate herding oil from multiple depressions to a single recovery channel cut into the ice where it can be removed from the water surface. If successful, this approach would reduce the number of recovery holes and ultimately the amount of time and effort required to remediate a spill under ice. Herein, we simulated a sub-surface ice depression using an acrylic sheet on top of a basin filled with water. Oil was injected into a pocket in the acrylic sheet and we assessed the ability of various air application systems to dislodging and relocating the entrapped oil (Tasks 1a). A field test was conducted using a salt water ice sheet with two sub-surface depressions grown at the Geophysical Research Facility (GRF) at CRREL. An underwater ROV was equipped with a camera for visualizing oil pockets under ice and the air application system that was most effective during lab trials. Oil was injected into the sub-surface depressions and we assess the ability of the retrofitted ROV to dislodge and herd the oil to a recovery channel cut into the ice sheet (Task 1b).

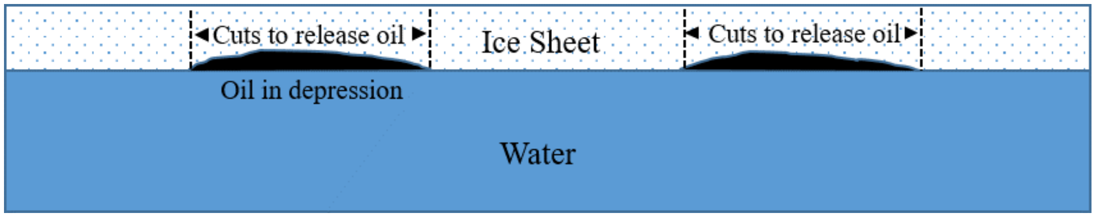

Figure 1.1. Theoretical cross-section depicting oil trapped in a depression under ice sheet.

Vertical Adhesion Belt (VAB) skimmers are a commonly used recovery method for removing oil from a water surface. The systems operates using an oleophilic adhesion belt that contacts the oil-water interface where oil sticks to the belt and is drawn up to the skimmer system for collection (Figure 3.1). In temperate conditions a VAB skimmer recovers oil/water mix at about 50:50 ratio. In low temperature conditions, ice may adhere to the belt, reducing the oleophilic surface area and its ability to recover oil. To mitigate this, we designed two heat application systems for the VAB skimmer and assessed their ability to attenuate icy build up in sub-freezing temperatures (Task 2a). The heat application system that performed best was further assessed using a simulated arctic oil spill scenario (Task 2b). Knowing the effectiveness of these heat application systems at various temperatures will allow responders to make informed decisions about their applicability during oil spill recovery efforts in sub-freezing temperatures.

As the temperature of oil decreases, its viscosity increases making it difficult to pump through a recovery hose and limiting its transferable distance. Additionally, as water is recovered with the oil, it may freeze further impeding the transfer process. The goal of this study was to design and test two in-line heat application methods, hot steam and electric heat pads, and assess their ability to improve performance of pump transfer of an oil-water mixture in sub-freezing temperatures. Additionally, we quantified the energy required for each system. With this data, we assessed if these heat sources would provide a viable method for mitigating pump failure in oil recovery activities in cold regions.

1.2 TASK DESCRIPTION

Specific tasks related to herding oil under ice (task 1), mitigating ice buildup during VAB skimmer recovery in sub-freezing temperatures (task 2), and improving transfer rate by reducing viscosity of oil-water mix during pumping (task 3) are described below.

Task 1: Herding oil under ice to a recovery location.

- ***Task 1a: Using air to dislodge oil from under an acrylic sheet and testing applicator configurations.***

A simulated ice sheet was developed using a 2.75 x 1.22 m acrylic sheet with a 17.75 cm diameter dome in the center to simulate a subsurface depression in an ice sheet. Alaskan North Slope (ANS) crude oil was injected into the dome and air was applied using applicators of different shapes and number of air holes. Using a grid on the acrylic sheet and cameras, we monitored the movement of the oil and air. With these data, we determined the applicator configuration that best guided the oil in the intended direction. Results of this test defined the optimal air applicator to be mounted on the underwater ROV for the field tests (task 1b).

- ***Task 1b: Field testing the ROV with air applicator under a salt water ice sheet.***

A 18.3 x 6.7 x 0.3 m thick salt water ice sheet was grown in the outdoor Geophysical Research Facility (GRF) at CRREL. Two 1m x 2m pockets were created under the ice to simulate sub-surface depressions. ANS crude oil was injected into both pockets. The ROV, fitted with air applicator, was submerged and an operator utilized the ROV's camera to guide it under the ice sheet while attempting to herd the oil from the depressions to a 1 x 1 m recovery hole cut into the ice sheet. The results of this test will define the applicability of herding oil under an ice sheet using an ROV with an air application system.

Task 2: Reduce ice accumulation on adhesion band of VAB skimmer operating in sub-freezing conditions.

- ***Task 2a: Assessing heat application systems abilities to reducing icy build up on adhesion band***

Tests were performed in a 3 x 3 x 1 m deep basin filled with salt water in the Material Evaluation Facility (MEF) at CRREL. A VAB skimmer system was fitted with a load cell to monitor changes in mass as ice accumulated on the adhesion band. The VAB skimmer ran continuously over the basin for 1h at temperatures of -10°C, -20°C and -28°C while icy build up was monitored. Then the VAB system was fitted with one of two heat application systems: 1. heat pads attached to the side of the metal skimmer and a foam insulated box that encapsulated the simmer unit; 2. a steam application collar around the adhesion belt located between where the belt exits the skimmer and enters the water surface. Each heat system was tested for one hour at temperatures of -10°C and -20°C and ice accumulation was monitored as a function of increasing mass on the system. The best performing heat system was further assessed using a simulated arctic oil spill senario in task 2b.

- ***Task 2b: Assessing how a steam application collar influences oil recovery rates for a VAB skimmer in sub-freezing temperatures***

Tests were performed in a 3 x 3 x 1 m deep basin filled with salt water in the Material Evaluation Facility (MEF) at CRREL. A 1 m^2 recovery area was created at the center and a VAB skimmer system was placed above the hole. Prior to each test, ice was allowed to accumulate on the adhesion belt. Then a continuous feeding system of ANS crude oil sustained a constant fuel slick thickness (2.5 cm thick) in the recovery area. Recovered oil was transferred from the VAB skimmer to a graduated barrel were we monitored recovery rates. The system ran for 1 h at -10 and -20°C to get an oil recovery rate baseline. At the same conditions steam was applied to the rope mop to determine how recovery rates were influenced. These results will define the efficacy of using a steam applicator to mitigate ice buildup on rope mops in sub-freezing temperatures.

Task 3: Mitigate the effects of cold temperature on pumping rates of oil and water mixture.

Two 300 gallon oil totes were used to supply and collect the oil-water mixture. An AL-50 Borger lube pump was used to pump the oil-water mix through a 200' long hose. Ten evenly spaced T-type thermocouples (TCs) were used to measure the mixture temperature along the length of the system. Various room temperatures of 0, -10, and -17 °C were used to determine the effects of cold temperatures on recovered oil pumping efficiency. The results of this test will define the efficacy of applying heat to pumping systems to increase pumping rate in sub-freezing temperatures.

CHAPTER 2 - HERDING OIL UNDER ICE

2.1 OBJECTIVES

Oil spilled under ice collects in the sub-surface depressions generated during ice formation, and over time can become encapsulated as the ice sheet grows. Depending on the time of year, response time may need to be on the order of hours to reach and extract the oil before encapsulation occurs. When released under ice, oil will quickly spread across multiple depressions. This makes recovery difficult using traditional mitigation techniques such as skimmers, dispersants, and in situ burning. New, more efficient methods to corral oil prior to recovery will reduce the amount of resources required and expedite oil recovery under ice. Alaskan North Slope (ANS) crude oil (779-917 kg/m^3) is less dense than salt water (1025 kg/m^3) and fresh water (1000 kg/m^3). Its buoyancy causes it to rest on the surface of water; however, when an ice sheet is present oil collects at the water-ice interface. Introducing a medium with a lower density, such as air (1.292 kg/m^3), into the depression may act as a barrier to separate the oil from the rough undersurface of the ice. Once the air fills the depression it will move to the next highest location under the ice sheet carrying the oil with it (Figure 2.1). In this study, we evaluated ability of compressed air to displace the oil from sub-surface depression and guided the oil to a recovery hole in an ice sheet.

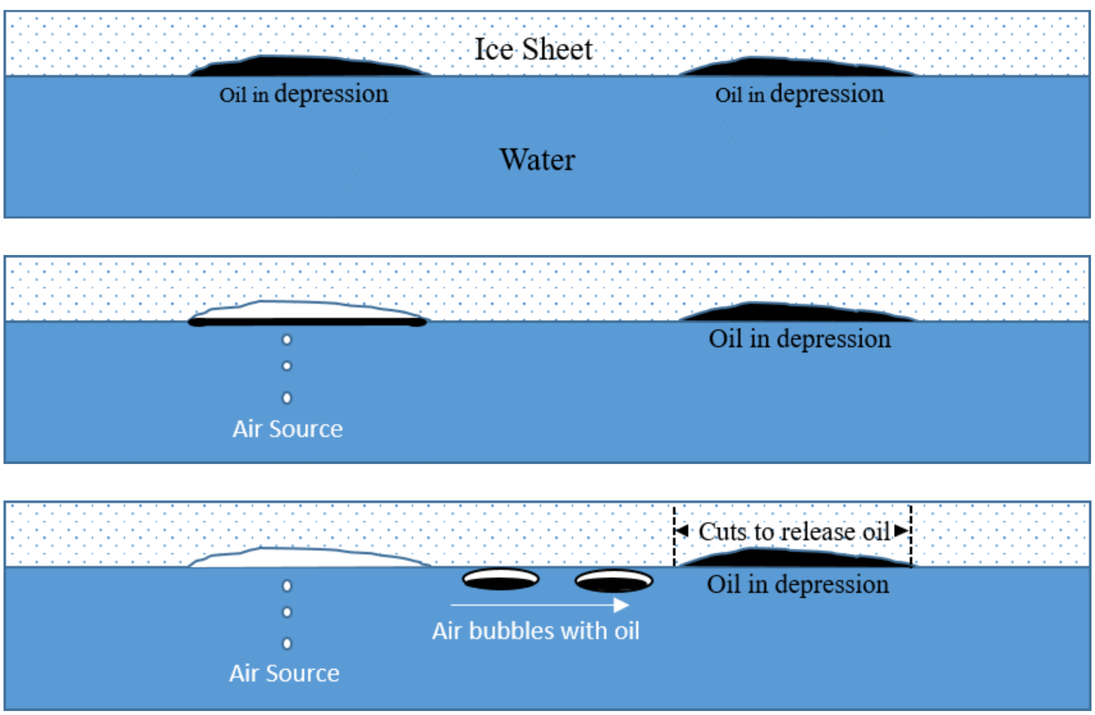

Figure 2.1. The theoretical cross-section of the interaction between supplied air, oil and water under an ice sheet. From top to bottom depicts oil trapped in sub-surface depressions of an ice sheet, air filling one

depression, and air relocating oil to another depression where oil could be recovered with a single cut into the ice sheet.

The herding oil with air technique was investigated in two phases. During the preliminary phase, we determined if oil could be manipulated and transported with air bubbles. Then we assessed an underwater air application system with various configurations to herd the oil to a retrieval point. In the second phase, an underwater ROV system was fitted with the choice applicator and assessed for buoyancy and directional control. A simplified oil spill under ice scenario was simulated by injecting oil into sub-surface depressions under an ice sheet. We assessed ability of the underwater ROV with air applicator to dislodge and herd the oil to a designated recovery hole cut into the ice sheet.

2.2 TRANSPORTING AND MANIPULATING OIL WITH AIR

2.2.1 Test Description and Setup

2.2.1.1 Moving oil with air under acrylic sheet

In a 3 x 3 x 1 m deep tank with a plastic liner (Fig. 2.2) a simulated ice sheet was created using a 2.75 x 1.22 m acrylic sheet framed with wood for structural stability and buoyancy (Fig. 2.3a). The sheet was manufactured with a 17.75 cm diameter dome in the center meant to simulate a sub-surface depression in the ice where ANS crude oil would be injected for testing (Fig. 2.3b). A 5 x 5 cm grid was drawn on the acrylic sheet to monitor the movement of the oil. To generate contrast between the oil and the background, white plastic panels were laid down and weighted to the bottom of the tank, and two underwater lights were installed. A hole was drilled in the dome, oil was injected with a 50-cc syringe, and the hole was resealed with electrical tape for testing. To dislodge the oil, air was supplied under the acrylic sheet via copper tubing in various configuration attached to an air compressor. A GoPro Hero 6 was place above the tank to monitor the movement of the oil and air during testing. Video footage was used to analyze the ability of air to dislodge and herd the oil.

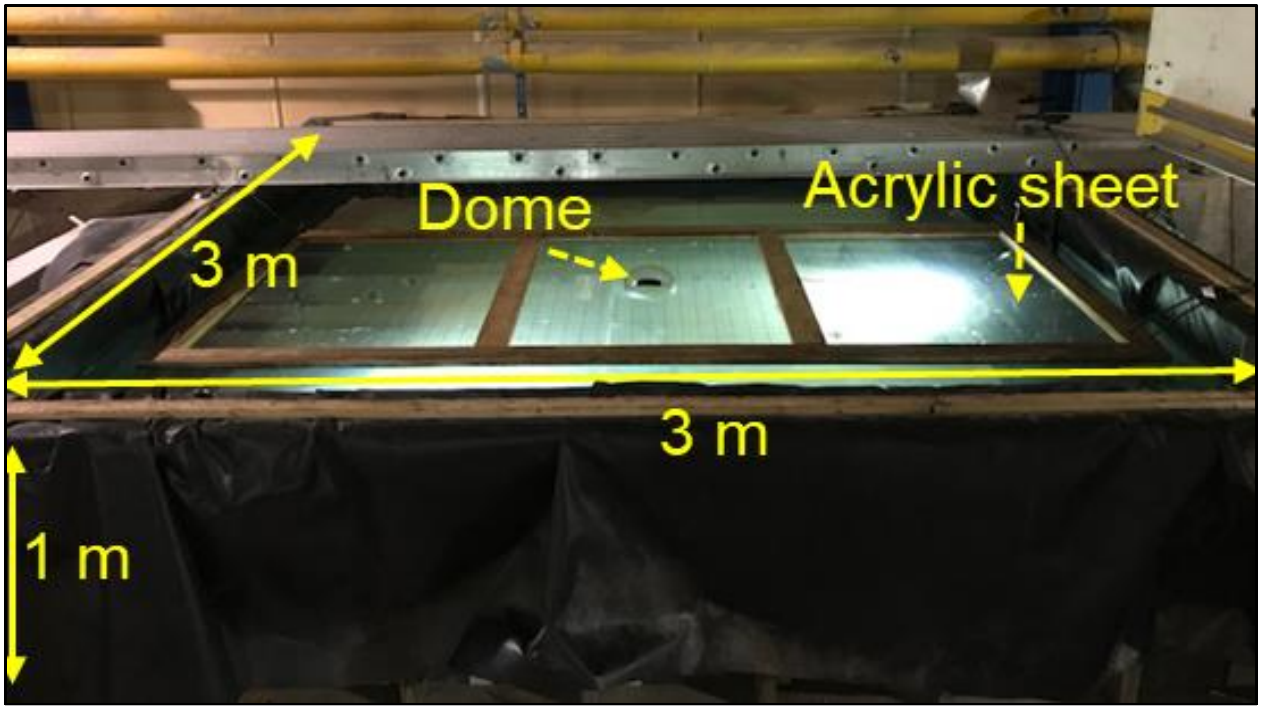

Figure 2.2. Tank used in preliminary tests with floating acrylic sheet used to simulate an ice sheet.

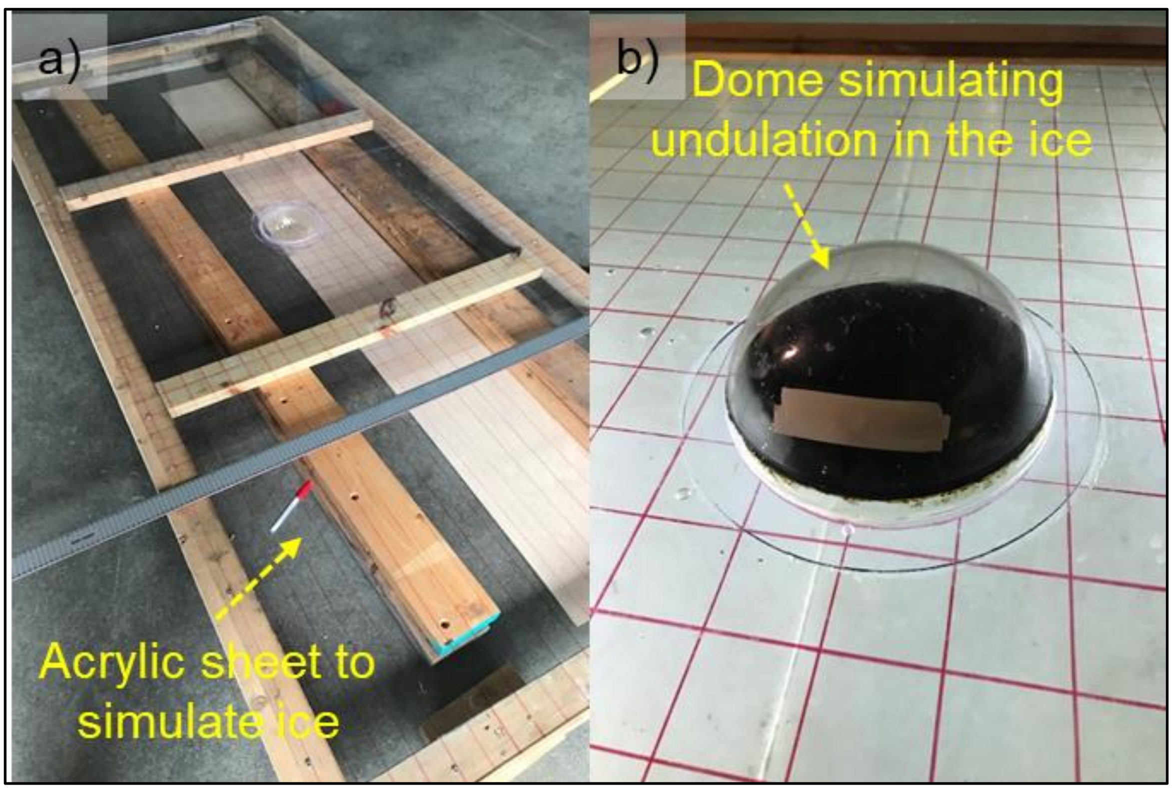

Figure 2.3. a) Acrylic sheet used to simulate ice, b) Dome simulating ice undulation

For the air injection system, the hose pressure was kept at ~15 psig (~103 kPa) for each air application configuration. This pressure supplied air rapidly enough to create a barrier between the oil and acrylic dome while keeping emulsification at a minimum. The air flow velocity and volumetric flow rate were calculated for each test nozzle. To do this, the air compressor was filled to a specific pressure. Air was released from the tank with the nozzle attached until the tank reached a specific end pressure. The time it took for the pressure to drop was recorded. By knowing the amount of air released via Boyle's Law (Eqn. 1), and assuming a constant temperature over a set amount of time, the volumetric flow rate was determined. Further, by knowing the hole diameter and number of holes in the copper pipe, the flow velocity could be determined.

$$PV = constant \qquad (1)$$

$$\frac{Volume}{time} = Volumetric\ flow\ rate \qquad (2)$$

$$\frac{[volumetric\ flow\ rate]}{area} = flow\ velocity \qquad (3)$$

2.2.1.2 Assessing Air Applicator Configurations

During the first round of tests, a metal applicator was created with a single air hole of 1.32 mm diameter. This used as a point source of air with the purpose of assessing how the oil moved when air was introduced into the dome. For the initial tests, the applicator was positioned directly below the oil trapped in the dome and air was applied. Then additional tests were performed with the applicator positioned at the edge of the dome in either the north, south, east and west locations.

For the second round of tests, a 1.1 m copper tube with a medial T junction was used to generate a bubble curtain. 1.32 mm diameter holes were drilled into the tube at 15 cm increments. This hole diameter size was selected to ensure bubbles were released consistently along the whole length of the pipe. The copper tubing was flexible enough to be manipulated into 3 test shapes to assess their efficacy. The shapes included a T, U and V configuration. The following test matrix describes the configuration and number of holes in the pipe that were used during each test.

Table 2.1. Test matrix for the Bubble Curtain Tests

Test #	1	2	3	4	5	6	7
Configuration	T	T	V	V	U	U	U
# of holes	4	6	4	6	4	6	8

2.2.2 Results and Discussion

The volumetric flow rate out of the point source applicator ranged between 0.042-0.47 m^3/min depending on the very slight difference in the hose pressure which results in a flow velocity of ~ 50 m/s. For the wand with 8 holes, the total volumetric flow rate was ~0.16 m^3/min with a flow velocity of 262 m/s per hole.

The initial point tests established that air effectively displace oil from a cavity. Regardless of orientation the oil was completely removed from the dome during each test (Figure 2.5). During the center test, the oil was pushed out of the pocket in in multiple directions. For the edge tests, the oil moves away from the air point source to the opposite side of the pocket (180 degrees). In all cases, the oil is initially emulsified due to the turbulence generated by the bubbles (Fig. 2.5, t = 6). In later frames the oil is being almost carried off, encapsulated by the air, away from the dome as seen in the north and west cases at time t = 12. The oil spreads out within the bubble as the air increases in surface area (Fig. 2.6).

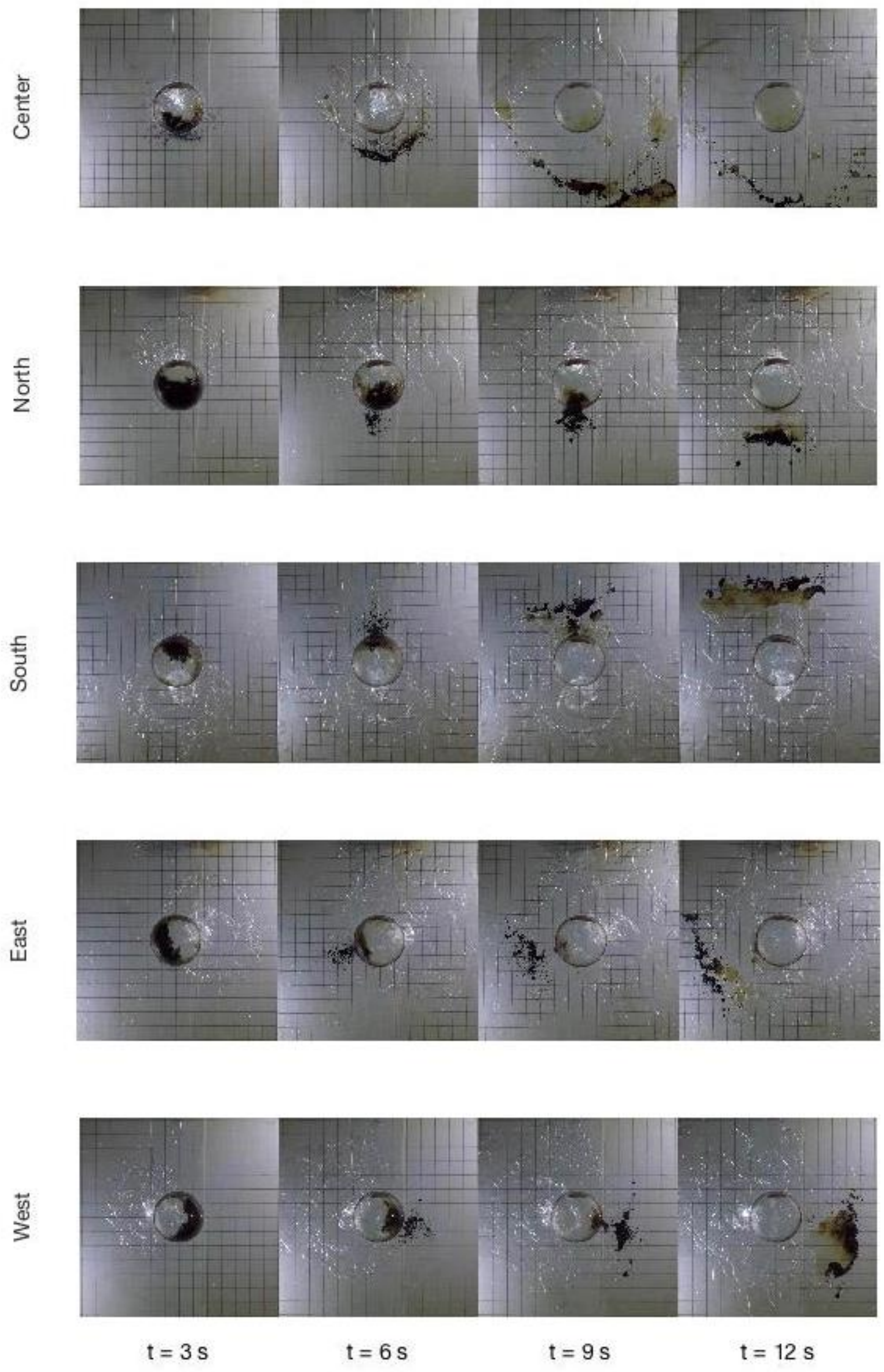

Figure 2.5. Results from point source air tests at five locations for time t = 3, 6, 9 and 12 seconds.

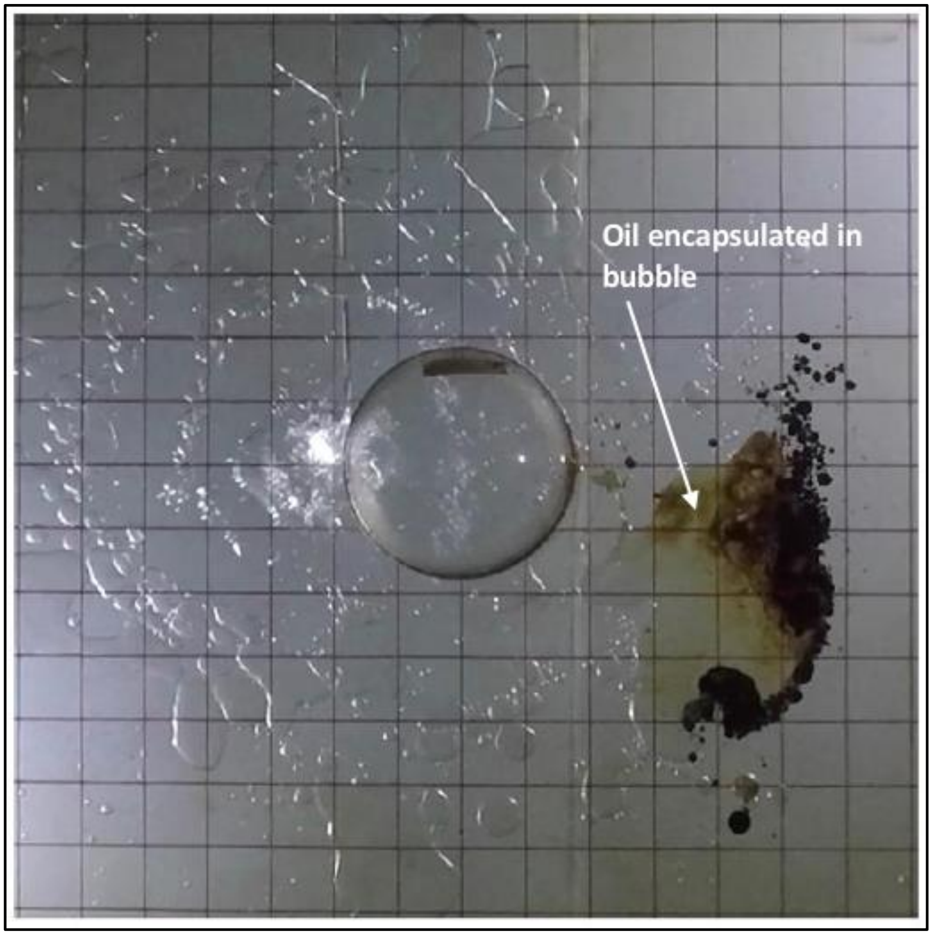

Figure 2.6. West point source test at time t = 12 seconds showing oil encapsulated in an air bubble.

The results of the bubble curtain testing indicated that spacing the holes at 15cm with a hole diameter of about 1.32 mm provided adequate air volume to prevent the oil from seeping through the air bubble curtain (Figure 2.7). The T attachment was capable of pushing the oil (Fig. 2.7), but as soon as the oil reached the edge of the pipe it went around the bubble curtain. Adding more holes to the applicator widened the effective bubble curtain, but did not prevents the oil from seeping around the edge. The V attachment behaved more like a point source due to the sharp bend in the copper pipe placing the holes closer together. Going from 4 holes to 6 holes improved the V shape by deepening the "pocket" of the V and was able to capture some of the oil as the pipe moved from one end of the sheet to the other. The U-shaped was the most successful at capturing and relocating the oil in the intended direction while keeping seepage to a minimum. Overall, the extended versions of each attachment worked more effectively compared to the shorter version. Therefore, the U-shape configuration with 8 air holes was selected for further assessment in task 1b. During all of the tests, due to the high volumetric flow rate, the air would quickly cover the bottom of the acrylic sheet and would seep out to the sides, pulling the oil with it. This impacted the test by limiting the amount of time the oil was actually under the acrylic sheet.

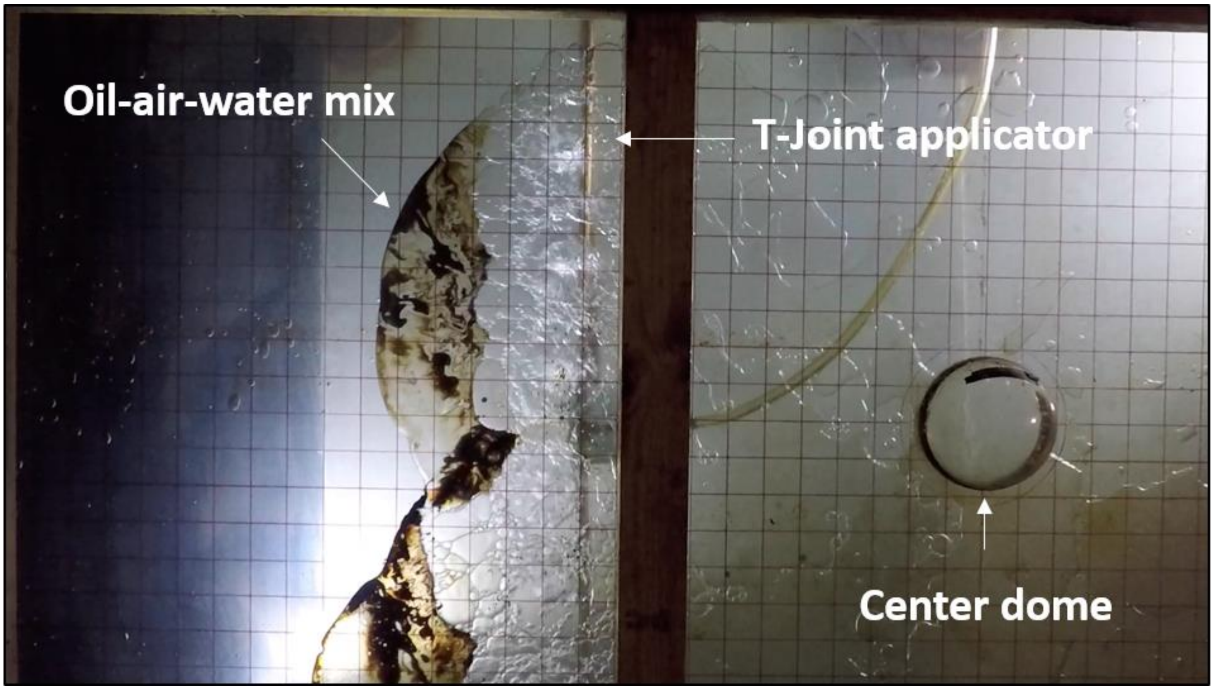

Figure 2.7. Oil being relocated from the center dome to the edge of the acrylic sheet by the T shaped air applicator containing 6 air holes.

2.3 HERDING OIL UNDER ICE WITH ROV

2.3.1 Test Description and Setup

The ROV buoyancy and control tests were conducted in the Test Basin a 37 x 9 x 2.4 m indoor concrete reservoir at CRREL. The ROV used for this testing was a LBV series manufactured by SeaBotix (Poway, California). The U-shaped air applicator was attached to the top of the ROV via zip ties. Underwater movement and stability of the vehicle was assessed within the Test Basin. After initial testing, blue-board Styrofoam was added to the ROV to compensate for the weight of the air application system.

Figure 2.4. Remotely Operated Vehicle (ROV) with air applicator attached.

The under-ice oil recovery tests were conducted in the Geophysical Research Facility (GRF) a 18.3 x 6.7 x 2.1 m outdoor basin at CRREL. The basin has a retractable roof that contains a refrigeration system able to maintain temperatures at 20°C below ambient to facility growing an ice sheet (Fig. 2.9).

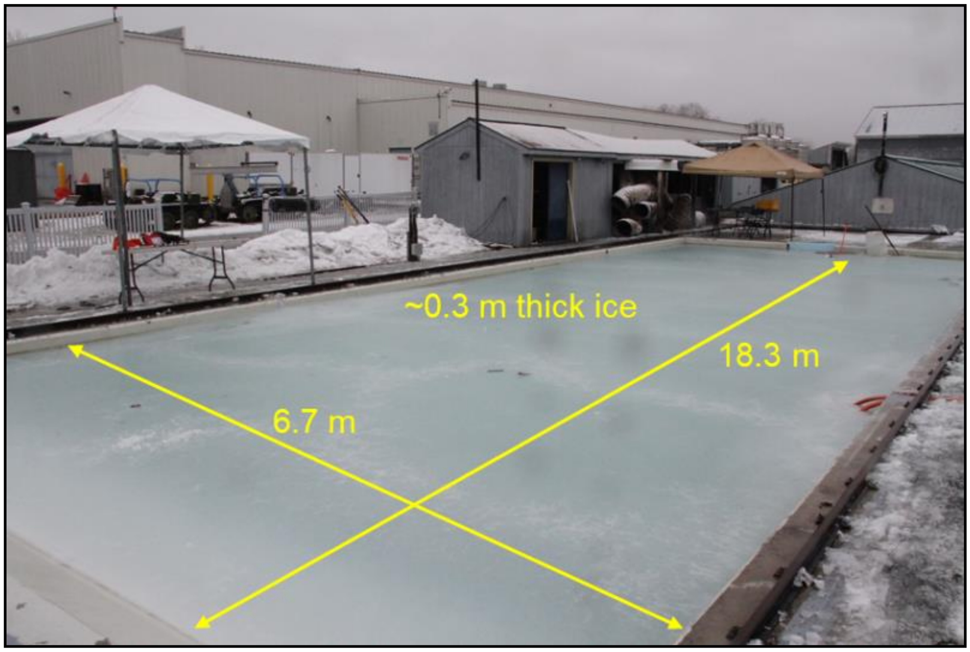

Figure 2.9. Geophysical Research Facility (GRF) used for large scale tests

A full demonstration of the bubbler herding concept was conducted under 30 cm of sea ice (salinity ~27ppt) in the GRF (Fig. 2.9 and 2.10). To create the subsurface depression in the ice 1 x

2 m blue board insulation panels at 5 cm and 7.6 cm thickness were placed on the ice sheet after it reached10 cm thickness. This slowed the ice growth directly under the boards relative to uncovered ice, resulting in a subsurface depression (Fig. 2.10a). Two holes, roughly 1 x 1 m in size, were cut into the ice for oil extraction and ROV deployment (Fig. 2.10c). Test was conducted under the ice on two separate dates. During the first test, oil was introduced under the ice via a pipe that was inserted through the oil extraction hole. Approximately 30 L of cold ANS crude oil was injected into the each subsurface depression (Fig. 2.10b). The injection of oil was monitored using an underwater GoPro camera mounted to the ROV. After injection, the oil was allowed to settle for approximately 15 minutes. The air compressor was turned on with a hose pressure of 15 psig, activating the air application system and starting the oil herding process.

For the second test a few modifications were made. In additional underwater GoPro was placed at the end of a pole for live viewing from a stationary position underneath the ice. The oil was injected at a slower rate to reduce emulsification for a cleaner pool of oil under the ice.

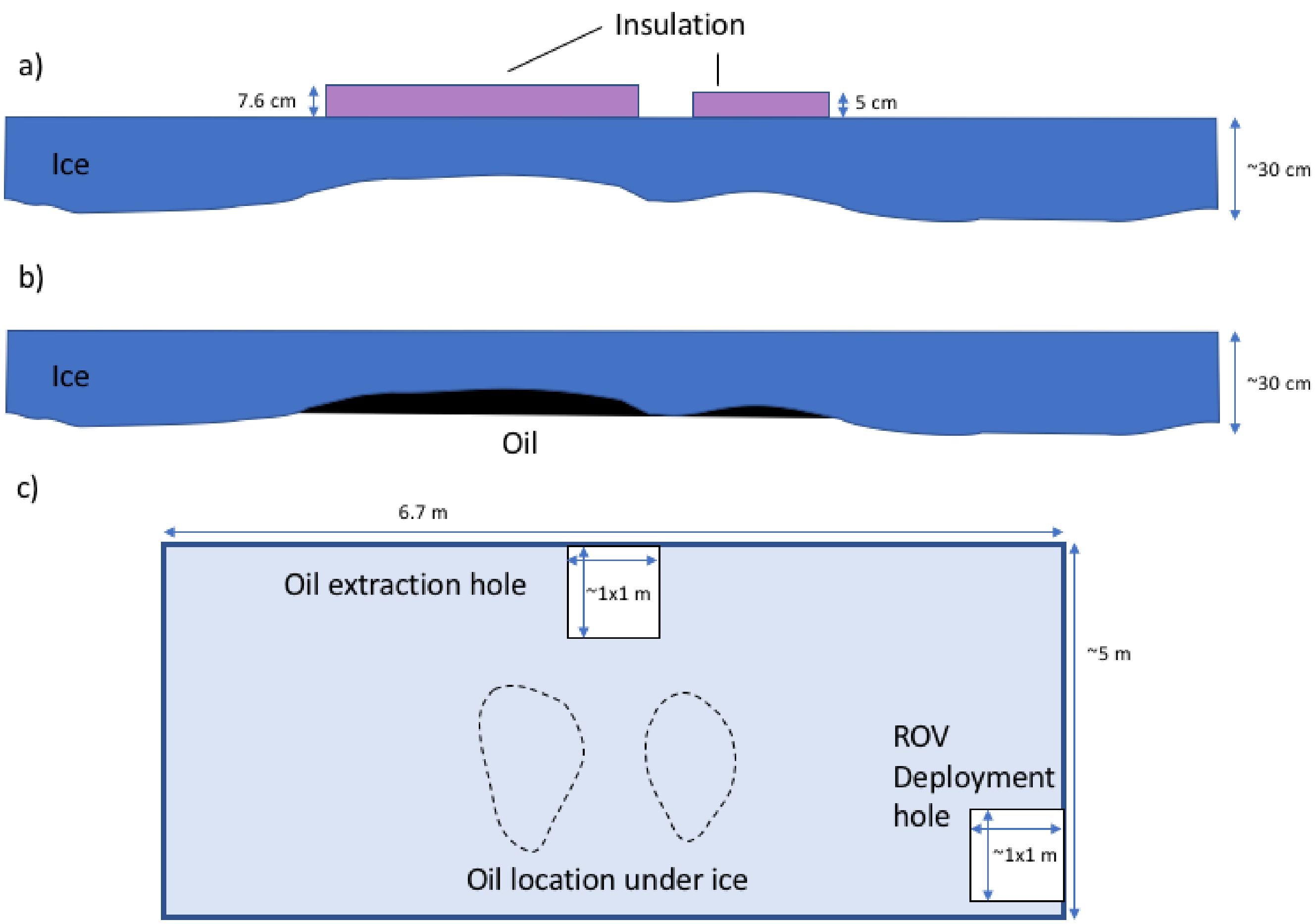

Figure 2.10. Layout of large scale-experiments a) Cross-sectional view of ice sheet, b) Oil trapped in undulations, c) Top view of the GRF.

2.3.2 Results and Discussion

When the bubbler was attached to the ROV and deployed in the Test Basin, the maneuverability and stability of the ROV was decreased slightly. It was observed that the bubbler system produced added drag by the hose, resulting in increased difficulty while stirring the ROV. The ROV also had trouble holding a steady depth position when equip with the air applicator system. This was cause by the weight of the air system and the downward thrush generated when air was flowing.

An unexpected result was observed during the testing. The air supply hose itself would float and create a barrier at the surface of the water (Fig. 2.8). It began trapping oil slicks and other materials floating in the pool. This could be utilized in some way in future investigations.

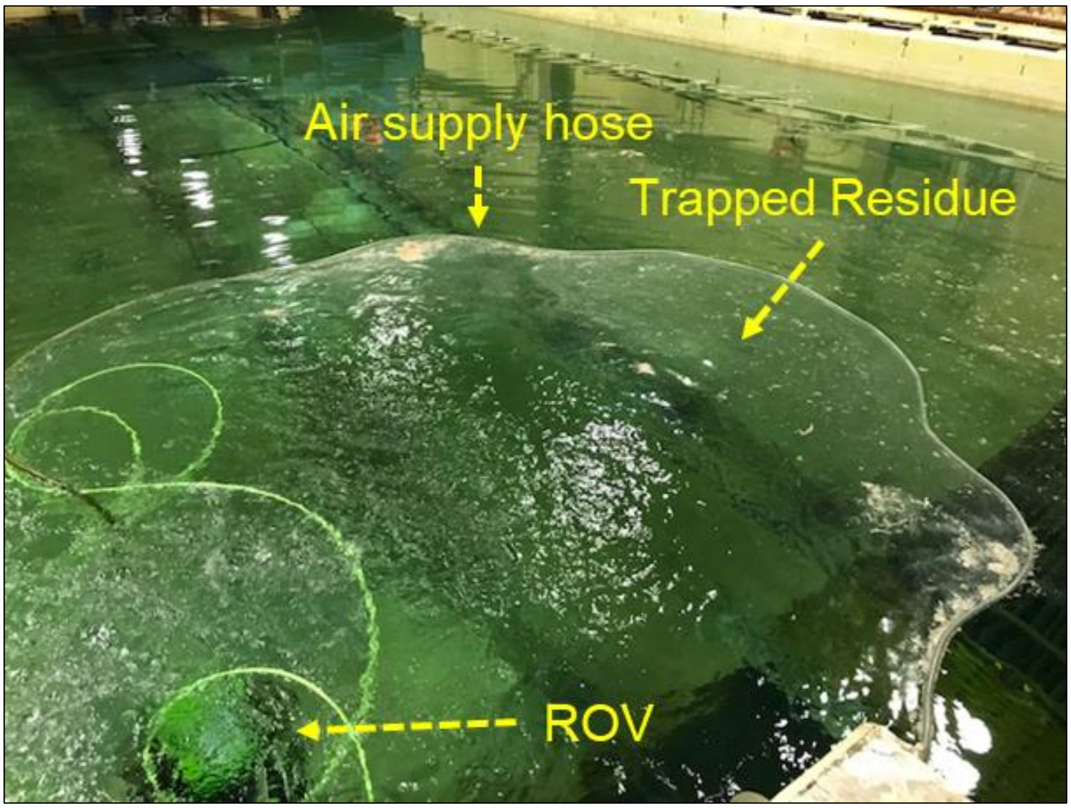

Figure 2.8. Trapped fluid by the air supply hose.

Each test under the ice sheet lasted about 30 minutes. The ROV was successful at introducing air into the oil filled depression and moving the oil to one side of the pocket. Once enough air was added to the pocket, it found the lowest edge to escape, and carried the oil with it. This made controlling the direction in which the oil moved very difficult and initially unpredictable. The ice sheet was bowed with the edges being higher/thinner compared to the middle. This resulted in the air and oil travelling to the edges of the ices sheet and not toward the recovery hole. It was necessary to cut an additional trench along the edge of the ice sheet to the facilitate oil recovery.

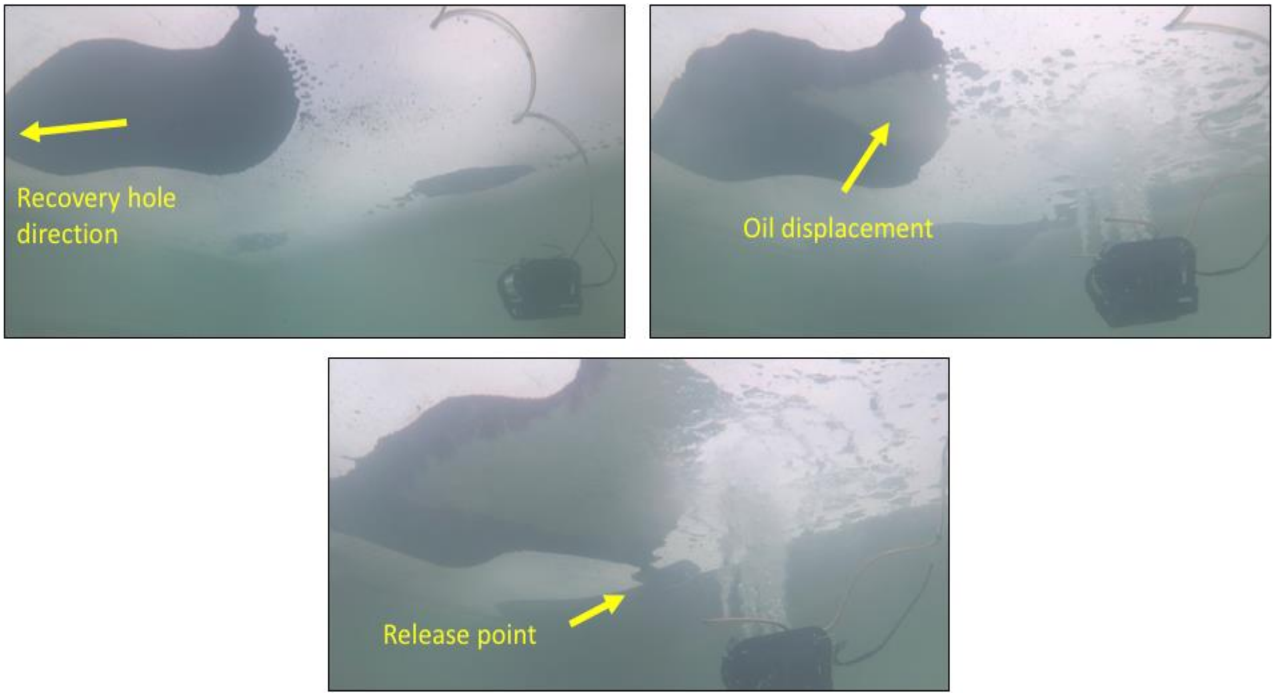

Figure 2.5. Under Ice Demonstration. (Left) oil trapped in a depression with air showing desired direction of movement to recovery hole. (Right) Oil being displaced by air towards recovery hole. (Bottom) Volume capacity of depression reached; air begins to escape with oil at lowest point towards the edge of the ice sheet.

The ROV was able to push the oil to a specific side of the air pocket, which provided evidence of some control in directing the oil. By injecting air off to the side of the oil, the air was less likely to stir up the oil and generate emulsion like it did during the preliminary testing. (Fig. 2.11, Right) It gently pushed the oil away from it as interface waves radiated away from the air source. The oil traveled with the air to the highest point in the bottom of the ice sheet (Fig. 2.11, Bottom) making it difficult to guide the oil to the intended recovery hole.

Figure 2.6. Fragile skeletal layer can be disturbed by compressed air action

After the tests were completed, sections of the ice were extracted to examine the underside of the ice. Figure 2.12 demonstrates the impact that the oil and compressed air had on the fragile skeletal layer. The warm oil/air mixture began to enter and expand the brine channels leading up towards the surface of the ice, and the bottom surface of the ice had clear streak markings from the compressed air blowing on it and the ROV occasionally bumping into the ice surface.

Overall, the ROV air application system was successful at dislodging oil form a pocket under the ice sheet; however, addition research is required to improve the ability to guide the oil to a desired location. For example, if the ice surface profile was known ahead of time, we could push the oil in the direction of the shallow ridge point until the air carried it out of the pocket. Future investigations should include a thorough recovery analysis to estimate efficiencies using this method. Additionally, investigating methods to reduce oil lost to ice entrapment during herding may lead to better recovery efficiencies.

CHAPTER 3 – ENHANCING ROPE MOP SKIMMER PERFORMANCE

3.1 INTRODUCTION

Vertical adhesion band (VAB) oil skimmers are a widely used technology for recovering oil from a water surface. VAB skimmers operate using oleophilic polypropylene fibers woven into to a looped rope that runs continuously through a skimmer system (Figure 3.1). The adhesion band is circulated through the oil water interface where oil collects on the band and is carried to the skimmer where rollers squeeze the liquid into an exit port for transfer to a collection reservoir. Although the adhesion band was designed to collect oil it also collects a small fraction of water. In subfreezing temperatures ice can accumulate on the adhesion band, drastically affecting its ability to recover oil. Some VAB skimmers are designed specifically for low temperature operation such as the recently developed Arctic Foxtail (H. Henriksen AS, Norway). However, the objective of this task was to developing a heating system that can be added on to a commercially available VAB skimmer and increase its ability to recover oil in sub-freezing temperatures.

Figure 3.1. FoxTail Mini vertical adhesion belt oil skimmer used in this project.

For Phase 1 of this study, we developed and assessed two heat application systems for their ability to attenuate ice accumulation on the adhesion band. This entailed a literature review of the current methods for applying heat to VAB skimmers. We selected an insulation and heating systems shown to be effective and feasible in field applications. Additionally, we developed a second heating system that utilized steam, a heat source typically available to arctic oil spill responders. Both heat application systems were assessed using a VAB skimmer that operated in simulated arctic condition for 1h as we monitored ice accumulation rates. The best performing heat system was selected for further assessment using a simulated arctic oil spill scenario. Appendix B describes the evaluation process of rope mop heating scenarios and the decision matrix that resulted in steam heat being the focus of phase 2 de-icing experiments.

For Phase 2 of this study, simplified oil spill scenario was created in the Material Evaluation Facility (MEF) that mimicked the conditions in which a rope mop skimmer would typically begin to accumulate ice and lose its effectiveness. The skimmer was equipped with a hot steam application system to heat the mop before it entering the oil-water mixture. Various tests with and without the heating unit were performed to determine the effect of heating on ice accumulation and oil recovery efficiency.

3.2 PROCEDURE AND SETUP

All tests were performed in a 3 x 3 x 1 m deep basin, filled with 32 ppt saline water (Fig. 3.1). A 1 m^2 recovery area was created at the center of the basin using a 15 cm deep metal containment pan. In the first phase of the project a FoxTail Mini skimmer (H. Henriksen AS, Norway) was cycled through salt water at subfreezing temperature. The skimmer was attached to a load cell (Figure 3.2a) to monitor ice accumulation rates as a function of increasing mass of the system. Then the skimmer was equipped with two separate heating methods, either an insulated casing or a steam generating collar developed by CRREL (Fig. 3.4) and ice accumulation rates were monitored. The steam collar was the most effective at attenuating ice accumulation on the adhesion belt and was used at the heat application for Phase 2. In Phase 2 oil tests investigated the change in oil recovery performance in the presence of the steam collar. In the oil recovery tests, a continuous feeding system (gravity feed) was used to sustain a constant fuel slick thickness (2.5 cm thick) in the recovery area for 1 hour while the VAB skimmer operated (Figure 3.2b).

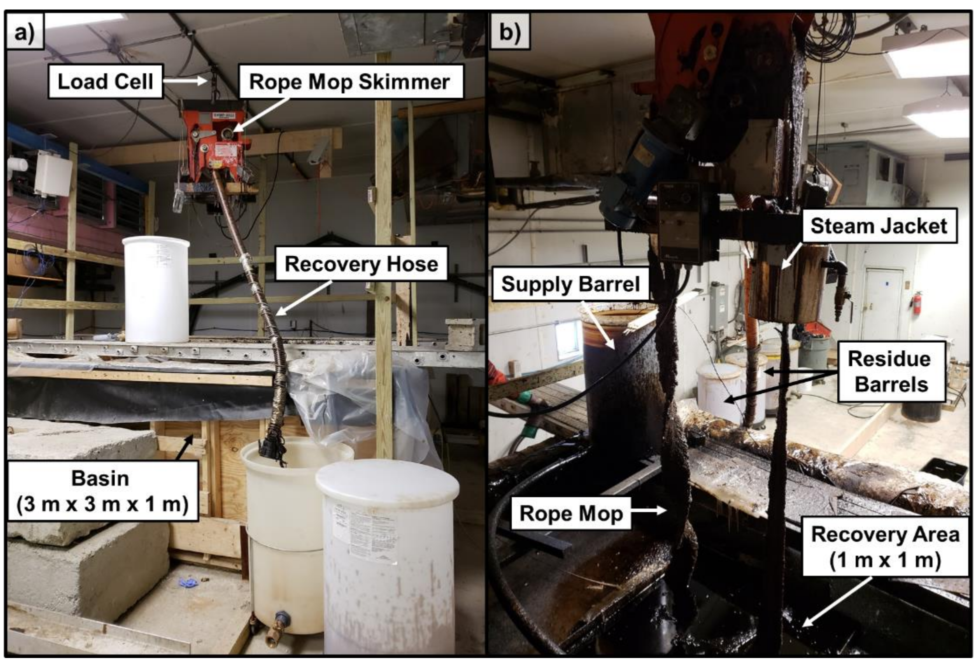

Figure 3.2. Experimental setup of the rope mop skimmer

Phase 1 (salt water): The adhesion belt was inserted into the skimmer and cycled through the salt water for 60 mins to get wet and cold. After 60 min, the experiment was started and ice accumulation on the mop was continuously recorded for an additional 60 mins. Ice accumulation was recorded as additional mass added to the skimmer during the experimental time interval and was measured using a load cell located at the top of the skimmer (Fig. 3.2a).

Figure 3.3 Image of insulated box with heat pads on VAB skimmer (*left*) and image of steam collar on VAB skimmer (*right*).

Phase 2 (oil on salt water): First, the adhesion belt skimmer operated in the salt water for one-hour to get wet and cold. Warm Alaska North Slope (ANS) crude oil was pumped into 55 gal drum in MEF and allowed to cool. When the oil temperature reached the water temperature (~1 ^{o}C), the experiment was started by introducing 7 gallons of oil (2.5 cm thick) into the 1 m^2 recovery area. The oil feed rate was adjusted to 1 gal/min and the skimmer was turned on. The skimmer operated at 9 m/min, the rate at which the maximum ice accumulation was observed during the salt water tests in Phase 1. The recovered fluid (water oil mix) was collected in 55-gallon barrels and the volume recorded in 5-minute intervals to calculate fluid collection rate (gal/min). At 10-minute interval the full/semi full barrel was change out for an empty barrel. For the steam collar tests, the hot steam jacket was turned on after 25 min of operation to apply steam to the adhesion belt. Hot steam was supplied from a Jenny Oil Fired Steam Cleaner system (Jenny Products, Inc) attached to an entrance port on the steam collar. At the end of the test, recovery barrels were moved to a warm area to enhance the oil-water separation. Water was decanted after 12 hours and the amount of oil in each bucket was recorded for oil recovery rate and efficiency. The oil recovery rate and recovery efficiency are calculated by the following equations.

ORR = volume oil collected/time

$$Recovery\ Efficiency\ = \frac{Oil\ left\ after\ decanting}{Total\ fluid\ in\ the\ barrel} \times 100 \qquad (1)$$

3.3 TEST MATRIX

Sixteen tests were performed to determine the effects of subfreezing temperatures on the VAB skimmer oil recovery rate. The first nine tests were performed with water only. A wooden frame was fabricated to sheathe the case of the Arctic Foxtail Mini. Two inch "blueboard" insulation was fastened to the wooden frame to create an effective insulation cover. Access ports were cut into the insulation to create hot steam injection points. The enhanced system was tested at -10 ^{o}C , -20 ^{o}C and -28 ^{o}C. Seven additional tests were performed with an oil slick to investigate the influence of hot steam on oil collection efficiency. Table 3.1 shows the test matrix.

Table 3.1. Test matrix for quantifying the oil recovery efficiency.

Room Temperature (^{o}C)	Heating Method	Oil Slick Thickness (cm)	# of tests
-10	N/A	N/A	1
-20			1
-28			1
-10	Insulation board placed on the skimmer case	N/A	1
-20			1
-28			1
-10	Hot steam applied on the adhesion belt	N/A	1
-20			1
-28			1
-10	N/A	2.5 cm	2
-20			1
-10	Steam Jenny		2
-20			2
		Total =	16

3.4 RESULTS AND DISCUSSION

3.4.1 Only Water Tests

Figure 3.2a shows the time vs. ice accumulation on the VAB skimmer at different subzero temperatures without the application of heating.

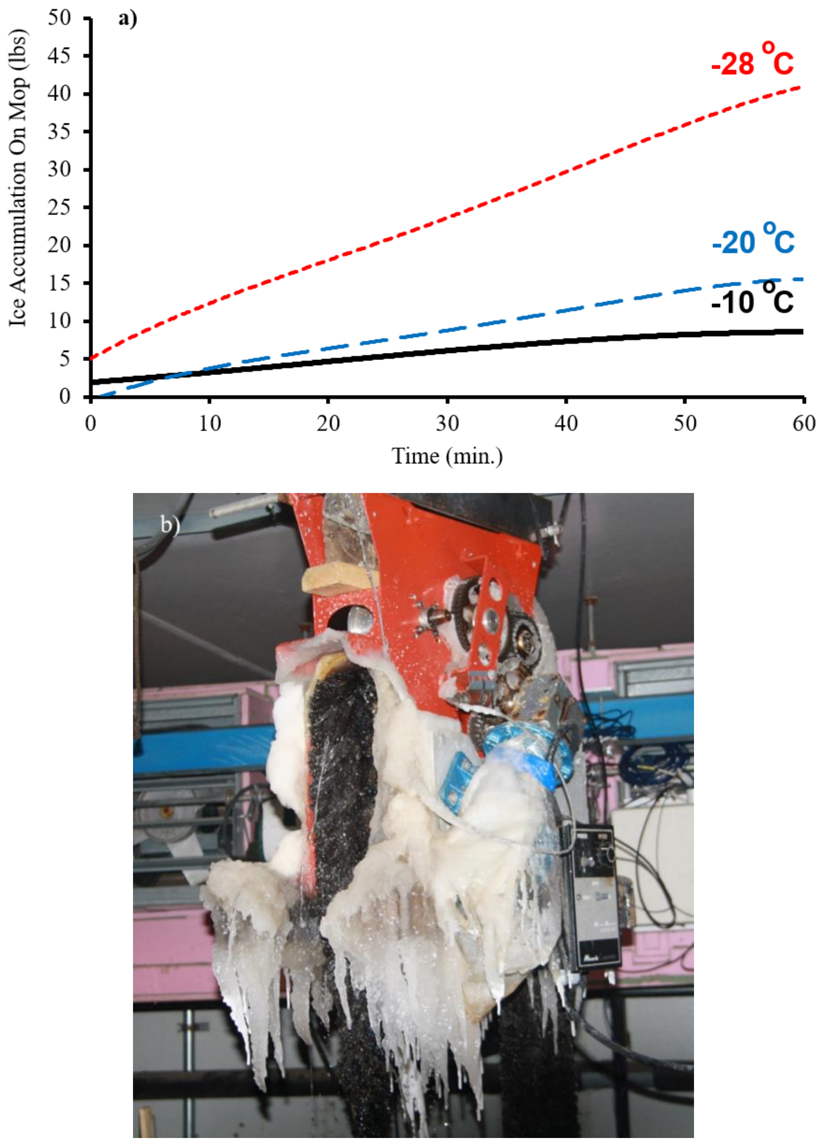

Figure 3.4. a) Ice accumulation on the rope mop at different subzero temperatures without the application of heating, b) Ice accumulation on the VAB skimmer and case at -28 °C after 1 hour testing.

As expected, ice accumulation on the rope and the skimmer case increased with time and decreasing temperature. At the end of the one hour experiment at -28C, approximately 19 kg (42 lbs) of ice had accumulated on the skimmer (Fig. 3.4a). Figure 3.2b shows the picture of the skimmer after testing at -28 °C.

Figure 3.4 shows the time vs. ice accumulation with different heating methods at -28 °C.

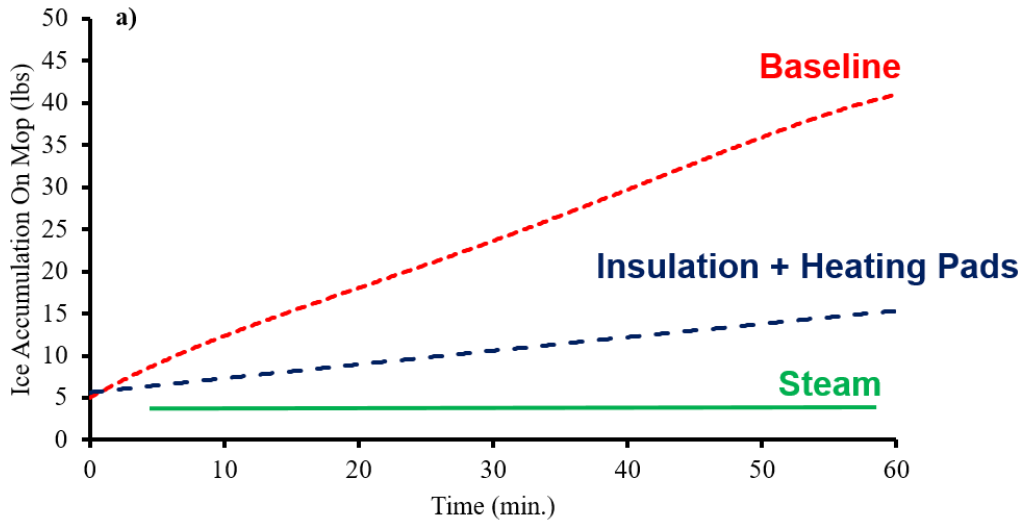

Figure 3.5. a) Ice accumulation on the adhesion belt at -28 ^{o}C with for the baseline (no heat), insulation and heat pads, steam collar heating methods.

As shown in Fig. 3.5, placing an insulation board and heat pads on the skimmer case decreased the ice accumulation by 66%, while the hot steam application prevented any ice accumulation on the rope mop. The hot steam application was further investigated by introducing oil into the system.

3.4.2 Oil Tests

Figure 3.6 shows the oil recovery rate and recovery efficiency of the rope mop skimmer at -10 ^{o}C.

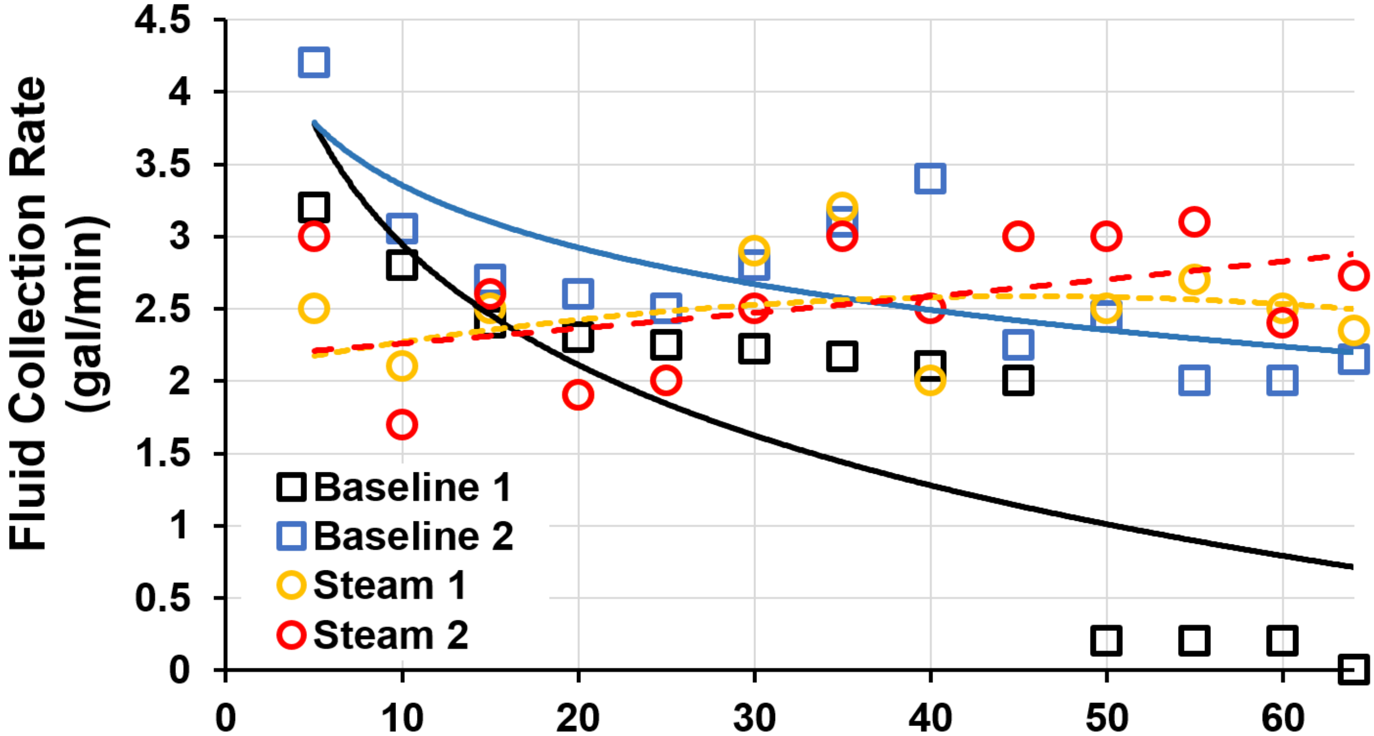
Fluid Collection Rate (gal/min)
4.5
4
3.5
3
2.5
2
1.5
1
0.5
0
0
10
20
30
40
50
60
Baseline 1
Baseline 2
Steam 1
Steam 2

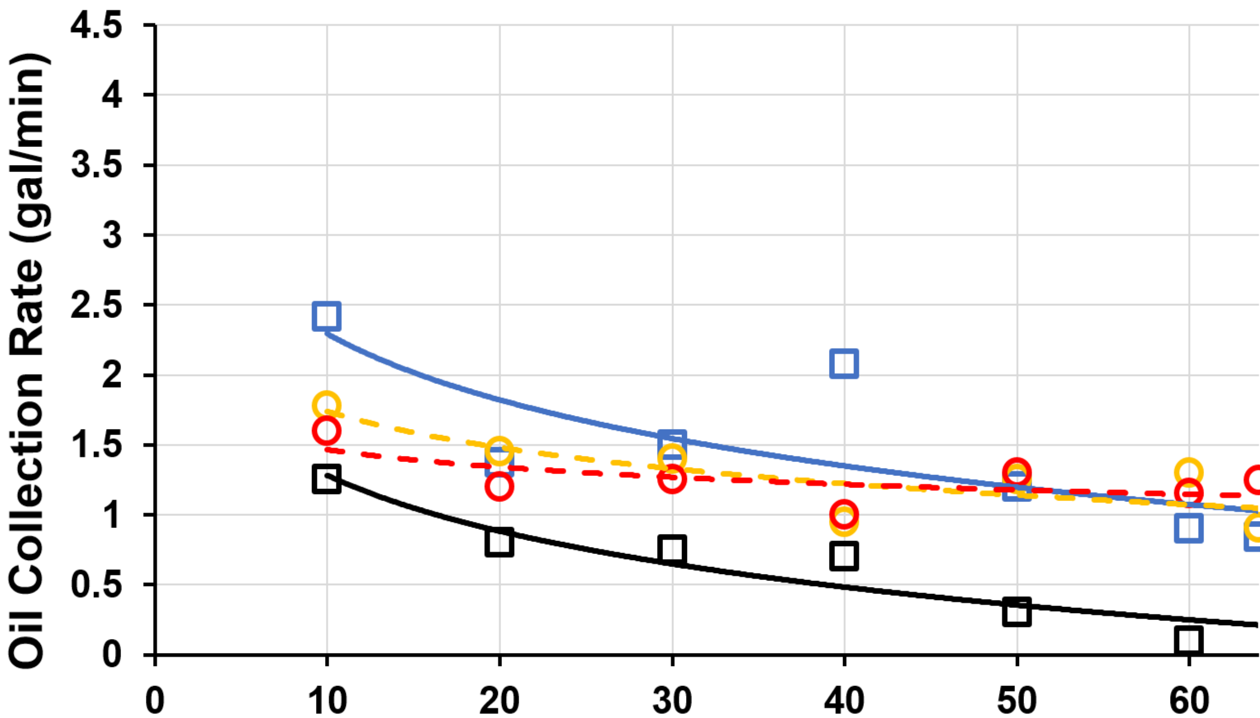
Oil Collection Rate (gal/min)
4.5
4
3.5
3
2.5
2
1.5
1
0.5
0
0
10
20
30
40
50
60

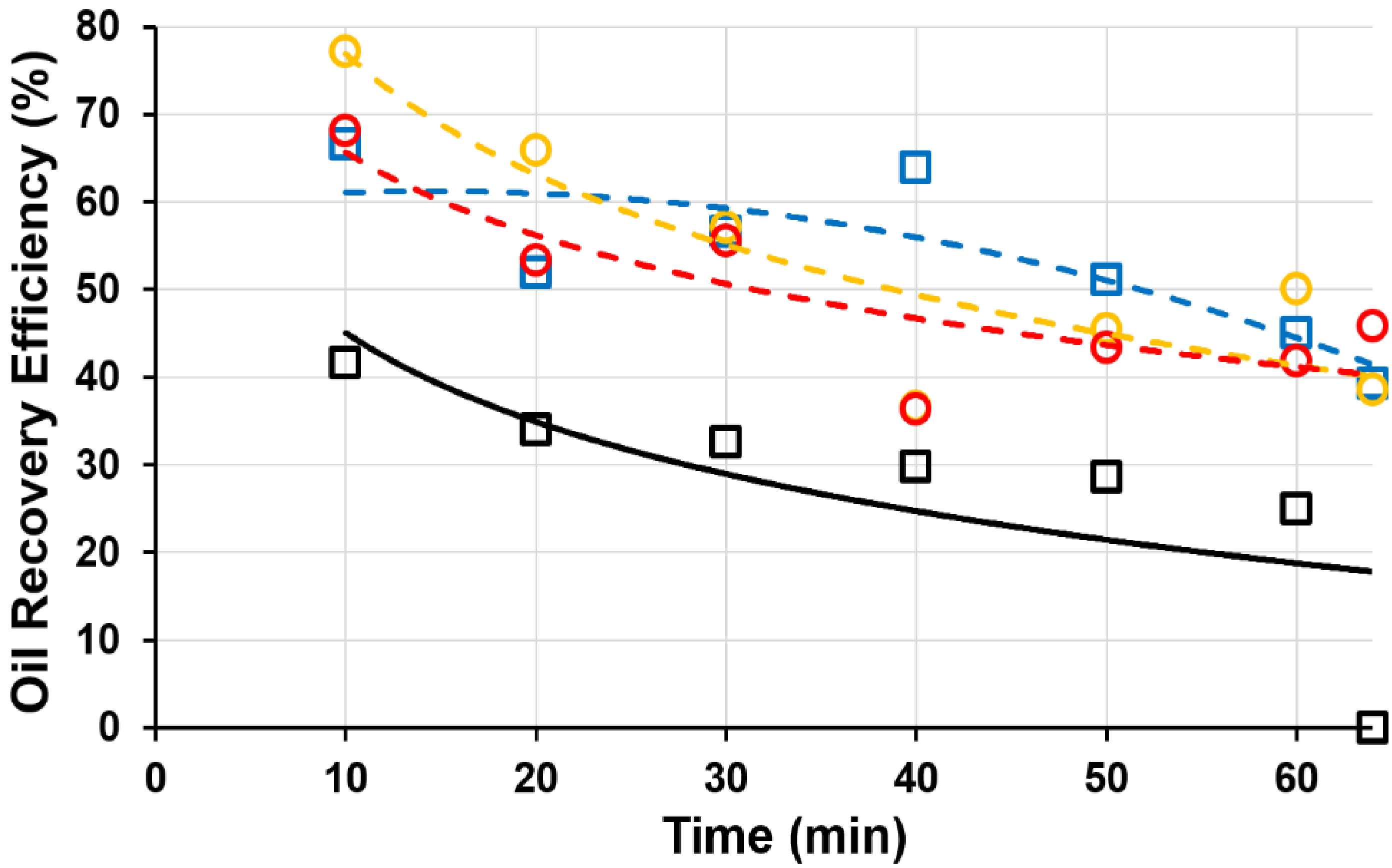

Figure 3.6. Fluid collection rate (water and oil), oil recovery rate, and oil recovery efficiency of the rope mop skimmer at -10 ºC. For the steam tests the steam collar was turned on at t=25 min.

As seen from Figure 3.7, the first baseline test performed at -10ºC failed at 45 minutes due to ice accumulation in the skimmer case. The flow from the recovery hose stopped and oil started to pour from the upper part of the skimmer (Figure 3.7). In order to prevent the same failure, it was decided to clean the skimmer case with hot steam each time before starting the tests. Although the second baseline started with a clean case, the decrease in fluid collection rate indicates ice accumulation and failure for longer operations. With the introduction of hot steam, the fluid collection rate started to increase. Initially the hot steam did not provide any enhancement on oil recovery efficiency. With the application of heat at 25 minutes, a sudden decrease in oil recovery efficiency was observed. At *t* is 40 minutes the recovery efficiency started to increase and become stable about 45% at *t* is 55 min., while it continues to decrease in the second baseline test (Figure 3.6).

Figure 3.7. Failure due to ice accumulation in the skimmer case.

Figure 3.8 shows the oil recovery rate and recovery efficiency of the rope mop skimmer at -20 ^{o}C. The baseline fluid collection rate drops from ~2.5 gal/min to ~2.1 with the decrease of the temperature. With the hot steam, the collection rate continues to decrease but becomes stable at the end of the test. The same drop in oil recovery efficiency was observed after applying the hot steam but at *t* is 35 min applied heat increased the recovery efficiency up to 58%. The expected benefit of the steam system is ice prevention and ice removal capabilities.

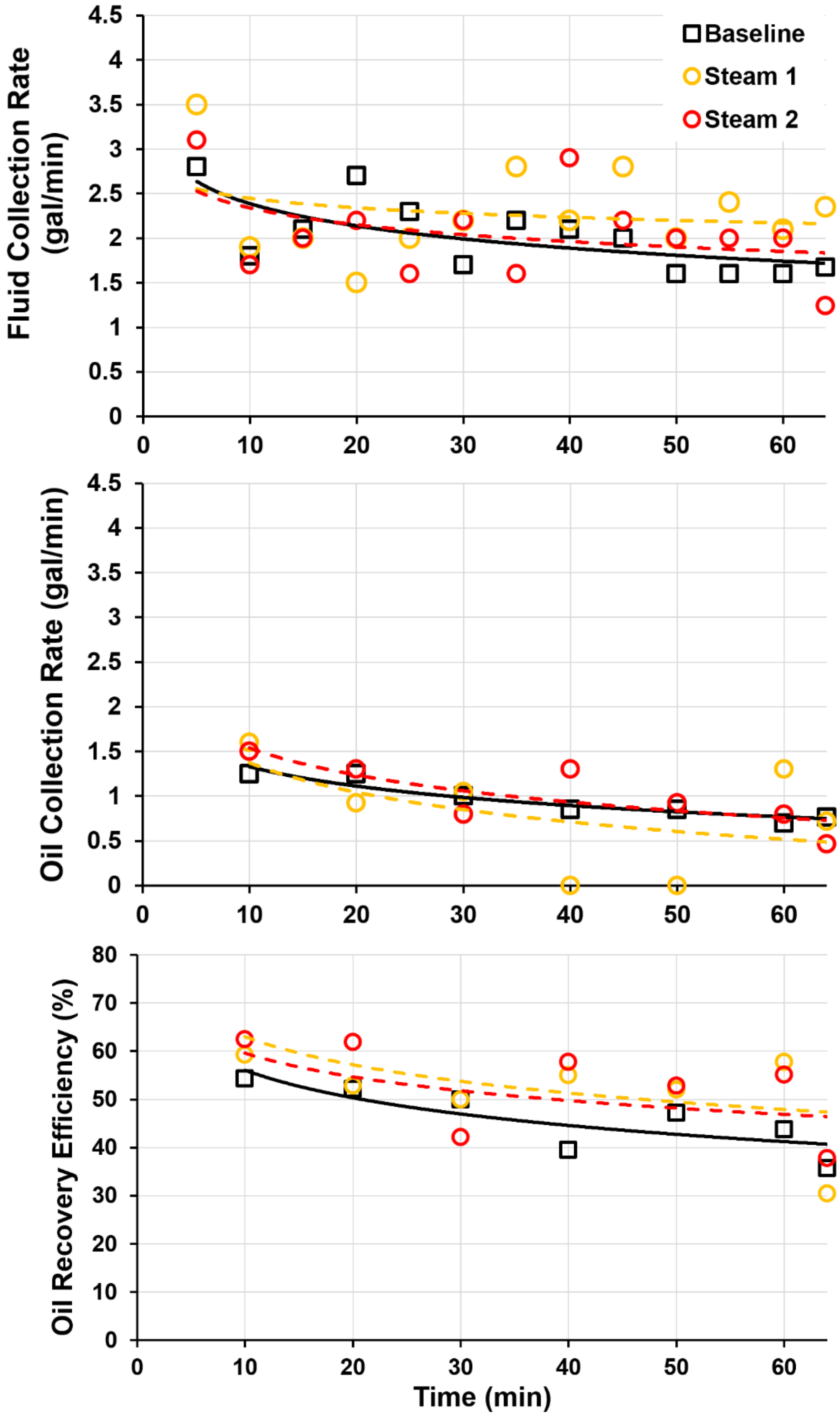

Figure 3.8. Fluid collection rate (water and oil), oil recovery rate, and oil recovery efficiency of the rope mop skimmer at -20 ºC. For the steam tests the steam collar was turned on at t=25 min.

CHAPTER 4 – HEATING OF RECOVERED OIL TO REDUCE VISCOSITY

4.1 OBJECTIVES

Oil recovered at cold temperatures has higher viscosity which may limit the distance that it can be pumped. At low temperatures, water recovered along with the oil may start to freeze within the recovery hose. In addition, if the temperature is lower than the oil's pour point, the oil may become "semi solid" and lose its flow characteristics. Cold Regions Research and Engineering Laboratory (CRREL) partnered with the Bureau of Safety and Environmental Enforcement in 2014 to assess how cold temperature impact oil pumpability using a hydraulic screw auger pump and a various lengths of hose (Campbell *et al*. 2016). Herein, we proposed to build on these results by development techniques to mitigate increasing oil viscosity in cold environments. The main objective of this study is to quantify the energy required to improve the fluid flow under low temperature conditions and compare it with the waste heat from generators and power packs used during oil spill mitigation procedures. Two methods, hot steam and electrical heat pads, were used to heat the oil as it was pumped through the recovery hose.

4.2 TEST DESCRIPTION AND SETUP

4.2.1 Pump System Setup

A simplified pumping system was created in the Material Evaluation Facility (MEF) at CRREL. The fluid used in this study was the oil-water mixture collected from the "Enhancing Rope Mop Skimmer Performance" tests. The mixture contained about 70% Alaska North Slope (ANS) Crude oil and 30% water. The tests setup is shown in Figure 4.1.

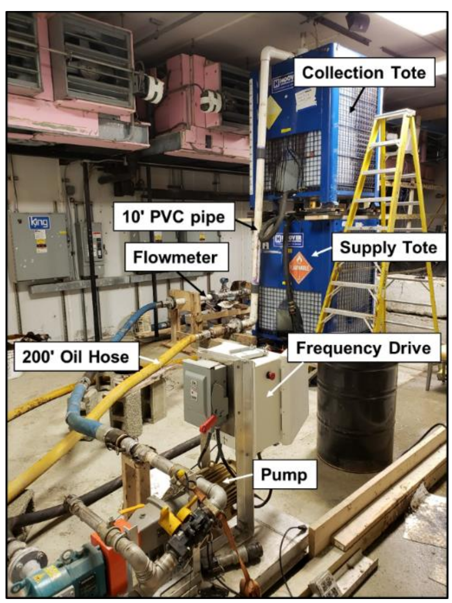

Figure 4.1. Experimental setup of the pumping efficiency tests.

Two 300 gallon oil totes were used to supply and collect the oil-water mixture. The collection tote was placed on top of the supply tote. Totes were connected with a 2” diameter hose that allowed the mixture to flow back to the supply tote by gravity. An AL-50 Borger lube pump controlled by a PowerFlex-400 Frequency Drive was linked to the supply tote. A wedge flowmeter equipped with a Rosemount differential pressure gauge (0-10 psi) and an absolute pressure gauge (0 to 100 psi) was used to measure the flowrate of the mixture. The pump cycled the mixture through the flowmeter, 200' long hose and totes. The end of the oil hose was linked to a 10' high head PVC Pipe mounted on the side of the stacked totes, which returned mixture to the collection tote. The return PVC loop eliminated the air pockets in the line. The mixture was pumped upwards through the 10' PVC pipe prior to being re-deposited into the collection tote to increase head pressure resulting in the flow meter registering a significant and measureable change.

Individual tests at a pre-determined mixture temperature (0 °C) and at three different room temperatures (0, -10, and -17 °C) were attempted for a period of one hour each. Ten T-type thermocouples (TCs) were used to measure the mixture temperature in the supply tote, pump, flowmeter, hose and collection tote. Mixture samples were collected from a port at the bottom of the 10' PVC pipe. A Brookfield viscometer was used to measure the viscosity of the collected samples. The frequency and the current drawn by the pump were also recorded.

Various issues were observed for the described test setup in cold temperatures:

- The water in the mixture froze in the thin pipes of the pressure gauges and caused malfunctions.
- The high viscous and frozen oil-water mixture blocked the gravity feed to the supply tote.
- Continuous cycling of the fluid dropped the mixture temperature and turned it into a slush, which was not pumpable.

In this context, the experimental setup and procedure was modified as follows:

- The supply and collection totes were unstacked.
- The mixture was pumped from supply to collection tote without cycling back. The test duration was determined by the pumping rate of 300 gal mixture at given temperature.
- Vehicle scales placed under the collection tote were used to measure the flowrates as a function of mass accumulation over time.

The modified test setup is shown in Figure 4.2.

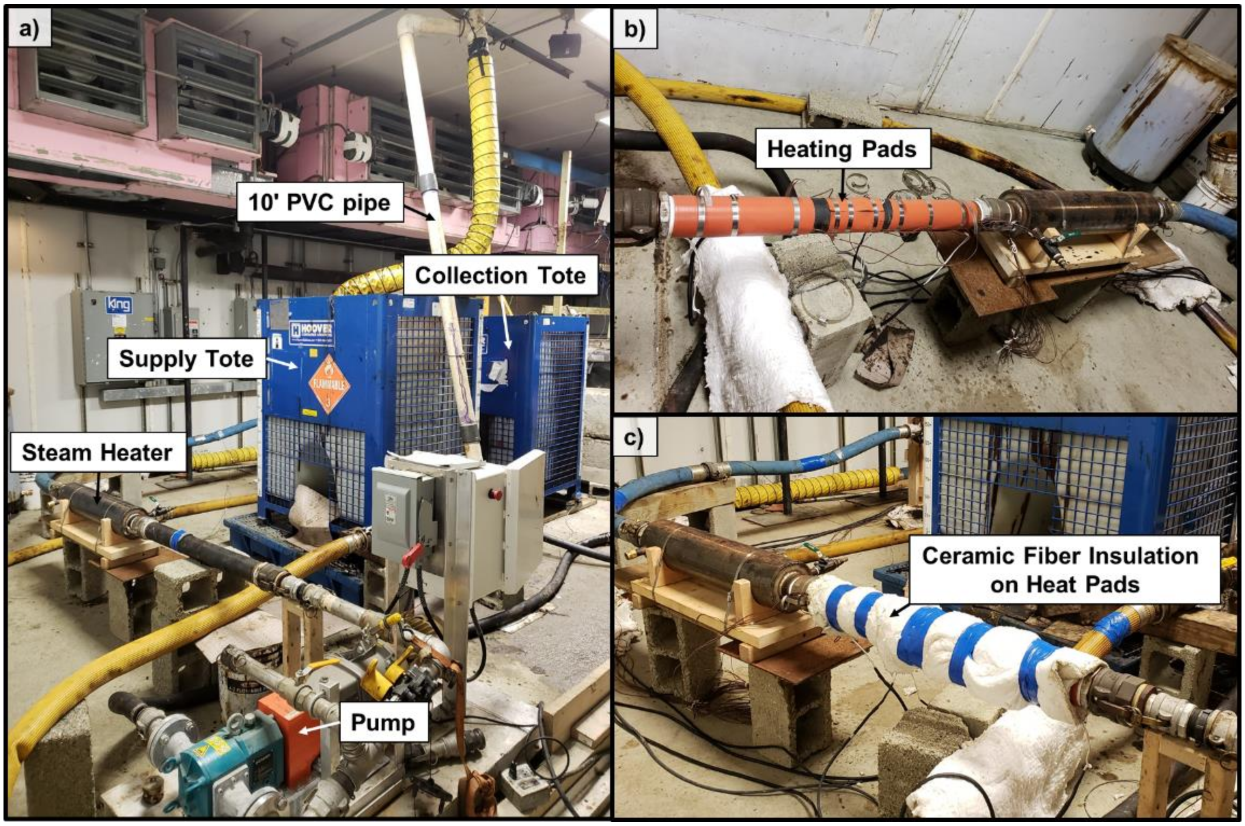

Figure 4.2. a) Modified experimental setup, b) Heating pads, c) Insulated heating pads.

The MEF was maintained at 8 °C when tests were not ongoing and dropped to the test temperature (0, -10, or -17 °C) a few hours prior to testing. This would prevent the fluid in the totes and hoses from freezing solid and blocking flow. When the temperature of oil-water mixture in the supply tote was at 0 °C and the room was at the defined condition, fluid viscosity in the line was recorded and the pump was turned on. Viscosity values and scale readings were recorded at every five minutes, while temperature, pump frequency and current data were recorded every 5 seconds. Testing continued until the supply tank was out of fluid. After the test, the room temperature was increased to 8 °C until the next test.

4.2.2 Heating Methods

Two heating methods including hot steam and electrical heat pads were investigated (Fig. 4.3). A steel steam jacket was manufactured by placing a 3' long 3" dimeter pipe in to a 3' long 6" diameter pipe and welding the edges together. The 3" diameter pipe carried the fluid while the 6" jacket contained the steam (Fig. 4.2a-b, Fig. 4.3a). 100 ^{o}C hot steam was supplied from a Jenny Oil Fired Steam Cleaner system (Jenny Products, Inc) attached to an entrance port on the jacket. Water generated form the steam was drained via an exit port and transferred outside of the MEF to eliminate freezing and blockage. Heat pad tests were performed by using four Choromalox (Two 12"x12" and two 6"x6") silicone rubber heaters with a maximum heating capacity of 200 ^{o}C (Fig. 4.2b, Fig. 4.3b). The pads were connected to an Omega CN1500 SERIES Multi-Zone Ramp & Soak controller. The controller maintained the temperature of the pads at 100 ^{o}C and recorded the current draw for each pad. To minimize the heat loss from pads to ambient, heating pads were covered with ceramic fiber insulation (Fig. 4.2c).

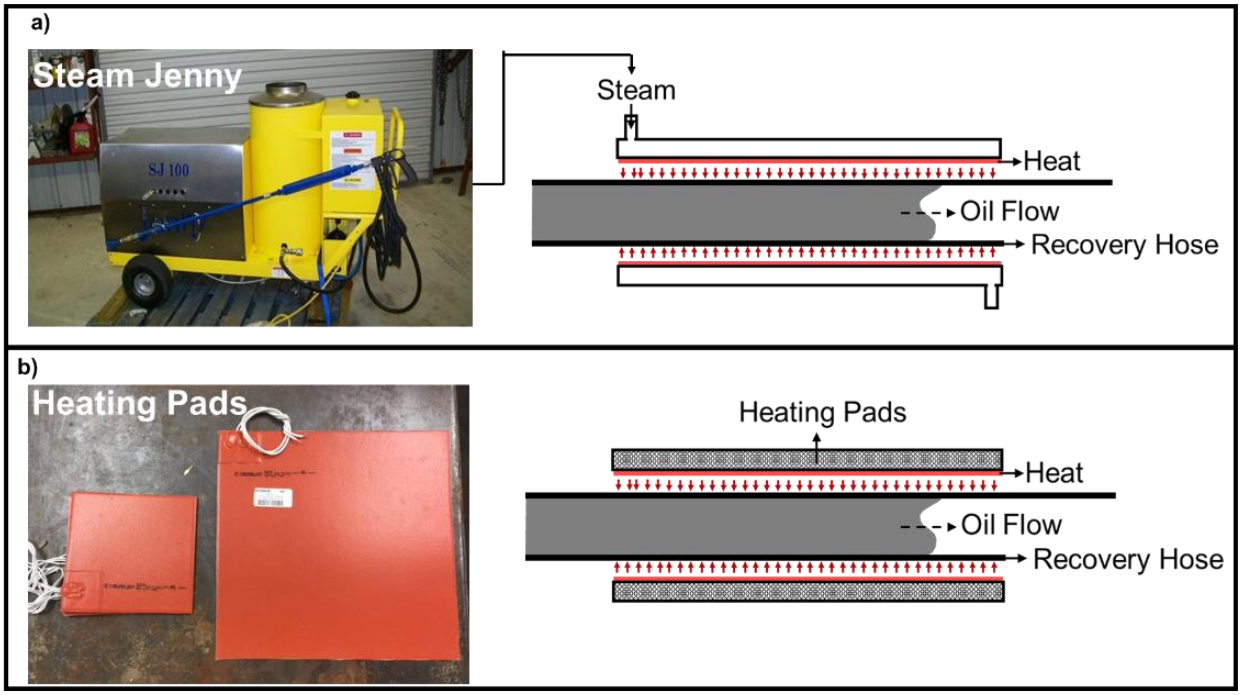

Figure 4.3. Tested heating methods a) Hot steam, b) Electrical heat pads.

4.3 TEST MATRIX

Fourteen tests were performed to quantify the effect of cold environment on pumping efficiency. Various room temperatures, such as 0, -10, and -17 °C were used to determine the effects of cold temperatures on recovered oil pumping efficiency. After the baseline tests, additional tests were performed to investigate the effects of heating on mixture viscosity, temperature and pump energy consumption.

Table 1. Test matrix to quantify the pumping efficiency.

Room Temperature (°C)	Heating Method	# of tests
0	N/A	3
	Electrical Heat Pads	1
	Hot Steam	1
-10	N/A	3
	Electrical Heat Pads	1
	Hot Steam	1
-17	N/A	2
	Electrical Heat Pads	1
	Hot Steam	1
		14

4.4 RESULTS AND DISCUSSION

4.4.1 Pumping Rate

Initial tests were conducted without a heating system (Fig. 4.4a). This set of tests showed a consistent flow rate, ~6 gal/min, through the experiments. At -17°C, a slow flow rate was observed at the beginning, ~3 gal/min. After 10 minutes, the flow rate reached to ~6 gal/min and remained constant. The same pattern was observed for the tests with hot steam and heat pads. We hypothesize that this pattern resulted due to the continuous mixing of the oil-water mixture at cold temperatures that caused emulsification. The high viscous emulsion (1200-1600 cp) sitting at the bottom of the supply tote was harder to pump than the oil-water mixture (100-600 cp) on top. As shown in Fig. 4.4 b-c, it took 15 minutes to pump the high viscous emulsion to the collection tote. Then the flow rate reached to ~6 gal/min while pumping the oil-water mixture.
It is shown that the 200' hose length was not long enough to see any variation in the fluid temperature and viscosity. Thus, the flow rate was similar for all cases.

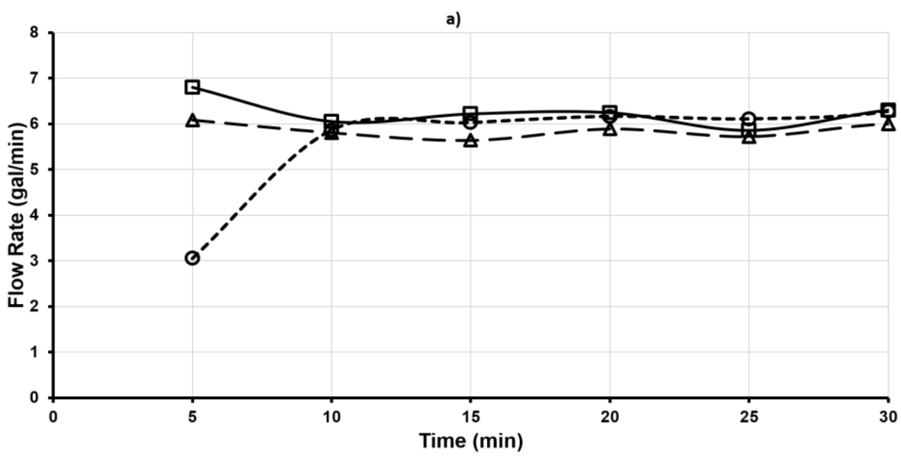

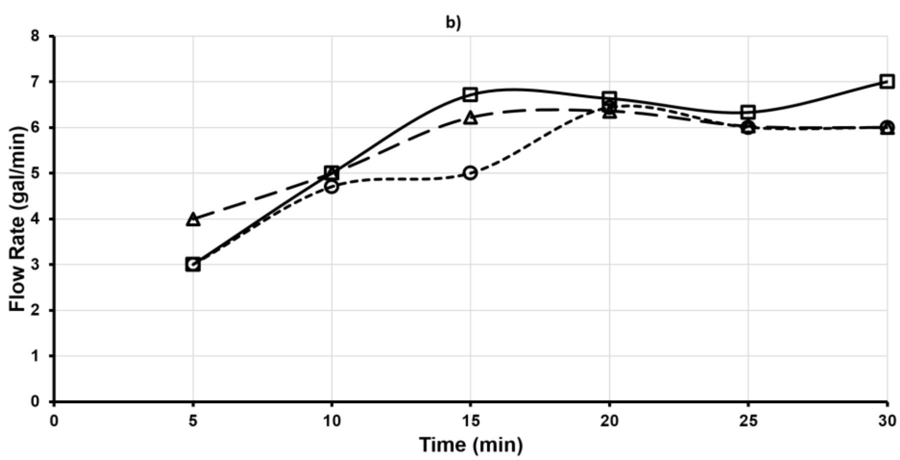

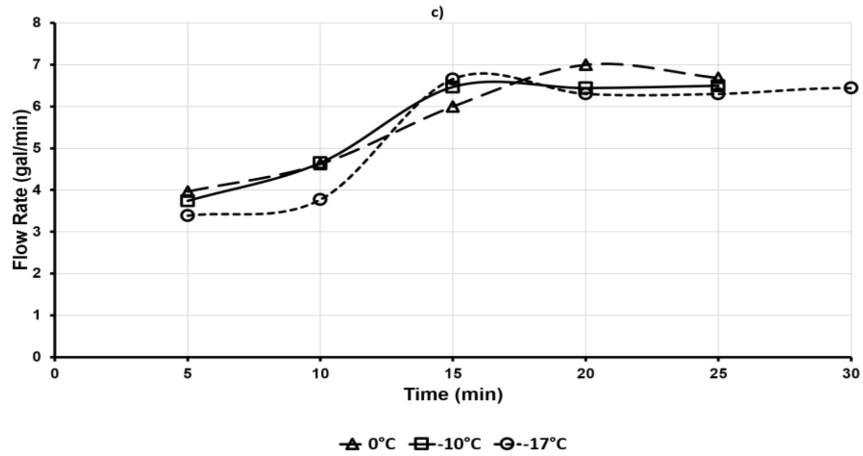

Figure 4.4. Flow rates at different temperatures a) No heating, b) Electric heat pads, c) Steam.

4.4.2 Temperature Transfer

TCs placed in the supply tote (0 ft), on the pump (10 ft away from the supply tote), heating section (13 ft away), flowmeter (16 ft), and the oil recovery hose (20, 45, 95, 145,195 and 220 ft) were used to measure temperature of the line. Figure 4.5 shows the temperature profile of the line at t=15 minutes of testing. The x-axis shows the distance from the supply tote in ft. Figure 4.5a shows the temperature profile at 0 ^oC for various heating methods. As expected, the oil-water mixture in the line remained constant at 0 ^oC without heating. With the introduction of heat pads, the temperature of the liquid inside of the heating pipe increased to 7 ^oC. The heat dissipated quickly in 7 ft and dropped to the room temperature at d = 20 ft (d is the distance from collection tote). The hot steam was able to heat the liquid up to 25 ^oC. The liquid remained warm until d = 145 ft (Fig. 4.5a). In -10 ^oC tests, the ΔT created by the heat pads and hot steam was 5 ^oC and 38 ^oC, respectively (Fig. 4.5b). The heat generated by heating pads was dissipated at d = 20 ft, while the liquid heated with hot steam remained warm until d = 95 ft. The hot steam outperforms the heating pads by creating a higher ΔT (~20 ^oC) and having a longer dissipation distance (d = 95 ft) (Fig. 4.5c). This data is useful to quantify the optimum spacing of the heating units. For example, hot steam needs to be applied every 130 ft for 0 ^oC ambient and 30 ft for subzero temperatures to protect the liquid from freezing. The spacing ensures that the liquid in the line does not drop below 0 ^oC. The detailed temperature profiles for the no heating, hot steam and heat pads at different ambient temperatures are given in Appendix A.

Hose length (x) required for the establishment of a fully developed temperature profile can be calculated as follows;

$$m = 6\ gal/\min = 3.7854\ \times 10^{-4} m^3\ /sec$$

$$U\ (velocity\ of\ mixture\ in\ the\ hose) = \frac{m}{A_{hose}} = \frac{3.7854\ \times 10^{-4}}{\pi \times 0.0762^2/_4} = 0.0830 m/s$$

Let’s check if the flow is laminar or turbulent.

$$R_e = \frac{\rho U D}{\mu} = \frac{UD}{\vartheta}$$

where ρ is the mixture density, D is the diameter of the hose, μ is the dynamic viscosity and ϑ is the kinematic viscosity of the mixture. If $R_e < 4000$ then the flow is laminar. If $R_e > 4000$ then the flow is turbulent.

$$R_e = \frac{0.0830 \times 0.0762}{1.78 \times 10^{-5} \text{ (The } \vartheta \text{ of crude oil at 20 °C)}} = 355, \text{the flow is laminar.}$$

Then $x = D \times 0.05 \times R_e \times P_r$
where P_r is the Prandtl number, which is 100 – 2000 for oils.

$x = 0.0762 \times 0.05 \times 355 \times 100 = 135\ m$
$x = 0.0762 \times 0.05 \times 355 \times 2000 = 2700\ m$

The results show that the hose length (x) required to drop the oil-water mixture temperature to the room temperature is between 135 -2700 m. Note that the calculations presented here are rough estimates. The P_r of the oil-water mixture should be known to calculate the x properly. Also, the ϑ of crude oil at 20 °C was used in the calculations. The ϑ should be larger in low temperatures.

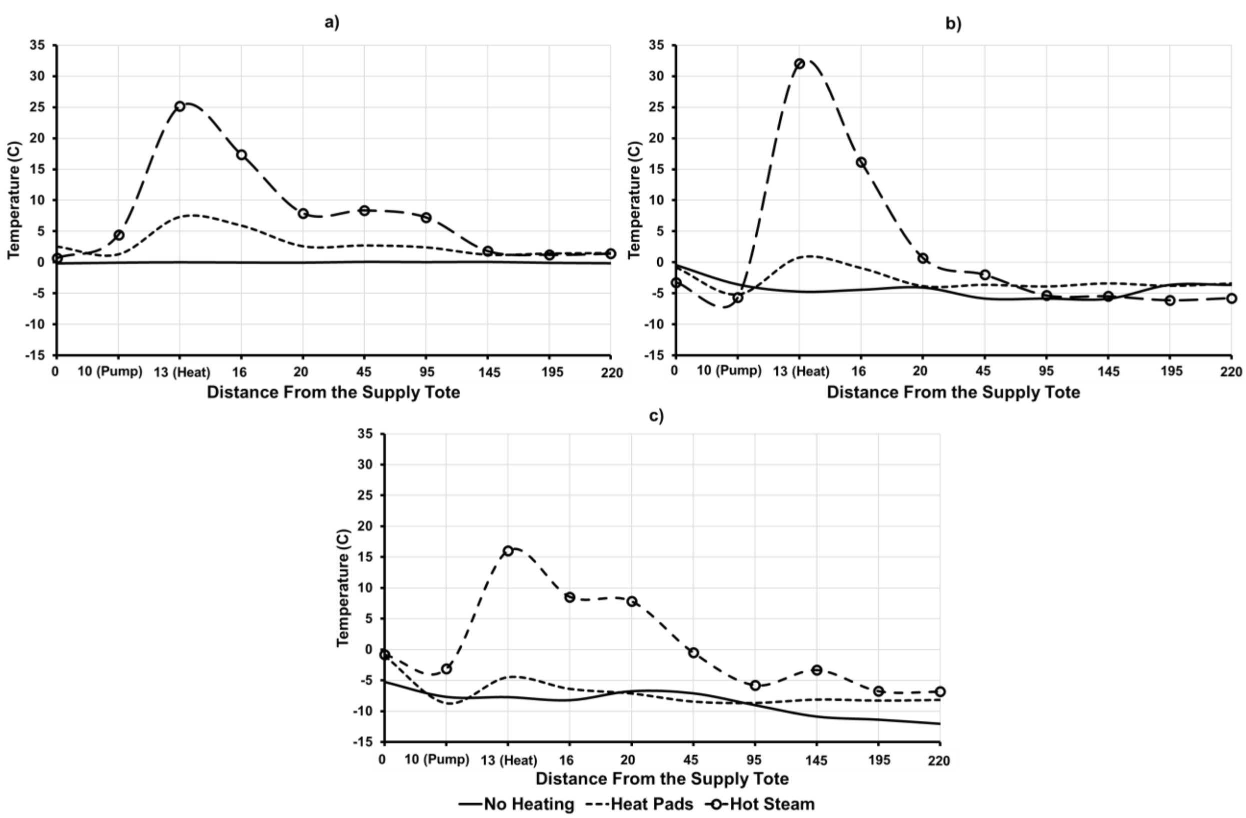

Figure 4.5. Temperatures profile of the line at t=15 minute a) 0 ºC, b) -10 ºC, c) -17 ºC. The x-axis shows the distance from the supply tote in ft.

4.4.3 Energy Consumption

The energy required to heat the fluid in the pipe to a certain temperature is calculated by the following equation:

$$Q = cm\Delta T$$

where Q, c, and m are the energy transferred, the specific heat capacity of the liquid, and the mass of the liquid being heated. ΔT is the change in temperature of the liquid. By knowing the ΔT from the test data and m from the flow rate, the energy transferred from the steam to the oil-water mixture can be calculated. The calculations for -10 ^{o}C is a follows:

$c_{ANS} = 2.3$ J/g°C [1]
$c_{water} = 4.18$ J/g°C [1]
$c_{eq} = (0.3 \times 4.18) + (0.7 \times 2.3) = 2.864$ J/g°C
$m = 6$ gal/min (From Fig. 4) $= 22712.5 cm^3/min \times 0.0008868$ kg/cm^3 $= 20.144 kg/min$
$m = 335.73 g/sec$
ΔT =33 – (-5)= 38°C (Figure A-e)
$Q = 2.864 \times 335.73 \times 38 = 36{,}538 J/s = 36.538$ kWh

To obtain the calculated energy, the steam jenny used 5 gal/hr of diesel fuel. The operation cost of the steam jenny for 1 hour is $12.87 (5 gal/hr x 2.574 $/gal*). To operation cost of the heating pads to obtain the same energy is $4.86 (36.538 kWh x0.1331 $/kWh). However, the results demonstrated that the heat pads were not effective to transfer the heat to the fuel (Fig. 4.5). The heat dissipated quickly and dropped to the ambient temperature in 7ft, while it took 140 ft for fuel temperature to drop ambient temperature with hot steam (Fig. 4.5b). That means heating pads need to be placed more frequent. 20 heat pads placed with 7 ft will be needed to achieve the same efficiency as one hot steam, which increases the operation cost to $98/hour.

*https://www.eia.gov/petroleum/gasdiesel/ last checked 8/26/2019.

CHAPTER 5 – CONCLUSIONS AND RECOMMENDATIONS

This project focused on improving oil spill recovery methods in Arctic conditions by developing and accessing techniques to herd oil under an ice sheet, increase recovery efficiencies of a VAB skimmer, and increase the pumpability of an oil/water mixture in sub-freezing temperatures. In Task 1 (Chapter 2) we showed that oil can be displaced and relocated from a sub-surface air pocket in an acrylic sheet using supplied air and we developed a U-shape air applicator attached to an underwater ROV for field use. We showed that the ROV and air applicator system successfully dislodge and relocated oil trapped under an ice sheet in a field test; however, we were not able to get the oil and air to move to a predetermined recovery location. We also found that warm supplied air may cause oil to become entrapped in the ice sheet. We recommend investigating how profiling an ice sheet to determine likely channels for passive air-oil flow prior to underwater ROV herding can influence the ability to move oil to an intend recovery location. We also recommend investigating how supplied air temperatures may influenced oil entrapment in an ice sheet.

In Task 2 (Chapter 3) we assessed the rate of ice accumulation on a VAB skimmer and showed that steam can be applied for attenuation. We developed a steam application collar as an accessory to VAB skimmers currently available on the market. We showed that while the steam collar can reduce ice accumulation on the adhesion belt it did not have a significant impact on oil recovery rates. However, it may prolong the ability of the VAB skimmer to recover oil in subfreezing temperatures. We showed that ice accumulates faster as temperature decrease; therefore, this system should be further tested in colder environments. We also recommend assessing incremental versus continuous use to reduce the amount of energy required to operate the system.

In Task 3 (Chapter 4) we showed that by applying heat to a steel pipe, we can increase the temperature of a flowing oil-water mix. We established the transferable distance of this heat through a commonly used oil recovery hose in subfreezing temperature. These data can be used to establish the frequency of this heating system required to ensure continuous heating of an oil-water mix being transferred through a hose. Pumping rates were not significantly influenced by the heating systems relative to the no-heat (control) tests. We concluded that this was due to insufficient hose length and cold temperatures to reduce pumping rates during the control tests. Therefore, future tests should include longer hoses and cooler temperatures. We also recommend investigating different oil-to-water ratios and the impact of weathering on oil pumping efficiency.

REFERENCES

1. Campbell S, Haskins KL, Winn, B, Stanley J, Zabilansky LJ (2014) Testing of Oil Skimmer Equipment Components for use in Arctic Environments. BSEE technical report.
2. Nixon, Z and Michel J. (2018) A review of distribution and quantity of lingering subsurface oil form the Exxon Valdez Oil Spill. Deep Sea Research Part II 147: 20-26
3. Torero JL, Olenick SM, Garo JP, Vantelon JP (2003) Determination of the burning characteristics of a slick of oil on water. Spill Science & Technology Bulletin 8(4):379-390.
4. Yang, S. Z., Jin, H. J., Wei, Z., He, R. X., Ji, Y. J., Li., X. M. and Yu, S. P. 2009. Bioremediation of oil spills in cold environments: A review. *Pedosphere*. **19**(3): 371–381.

APPENDIX A

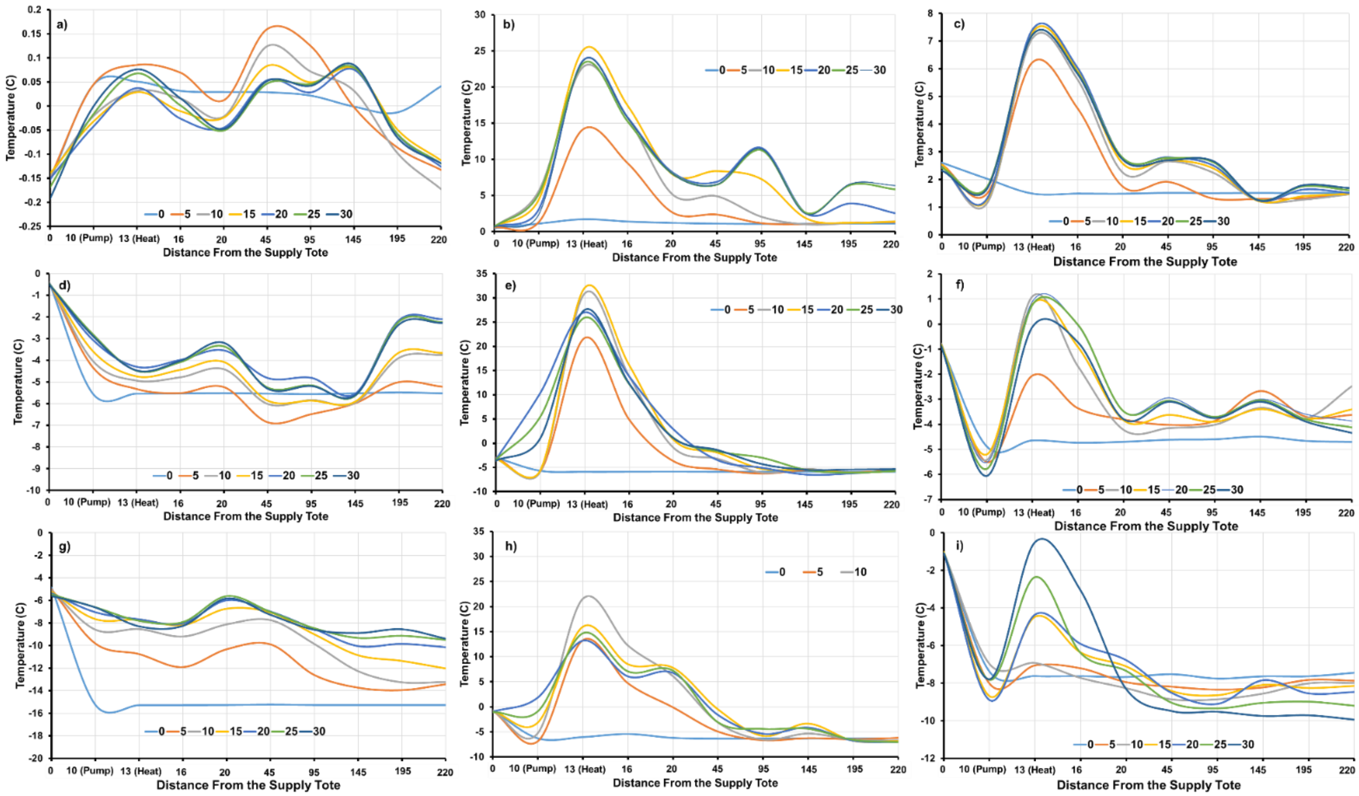

Figure A. Time history of the oil-water mixture temperature through the line with 5 min time intervals, a) 0 ^{O}C-No heating, b) 0 ^{O}C- Hot steam, c) 0 ^{O}C-Heat Pads, d) -10 ^{O}C-No heating, e) -10 ^{O}C- Hot steam, f) -10 ^{O}C-Heat Pads, g) -17 ^{O}C-No heating, h) -17 ^{O}C- Hot steam, i) -17 ^{O}C-Heat Pads.

APPENDIX B

Heating Requirements for a Foxtail Rope Mop Skimmer:

Prepared by

Nathan Lamie

US Army Corps of Engineers

Cold Regions Research Engineering Laboratory

Dec. 30 2016

Challenge: Apply heat in, some form, to a rope mop and determine how much heat and how far away that heat source would have to be in order to heat the mop without damaging the material. Additionally spec-out heaters (IR, heat tape, mats) that might be appropriate to heat the mop. Some options for heating include: heat tape on the pulleys and ringers for the mop, once the oil has been cleaned off the mop possible heating strategies are: heat-tape within a pipe that the mop passes through, a duct with forced heated air that the mop passes through, steam heating of the mop just before it enters the water.

The first and most pressing set of questions are:

- What is the temperature of the rope mop?
- How much does the temperature of the mop need to be raised in order to reach an ice-resistant state?

Following the answers to these questions:

- What are the heating requirements to reach the desired temperatures?
- What heat sources meet these requirements?
- What are the distances needed for the mop to be from these heat sources to provide this heat but not damage the material?

Specifications of the Foxtail Mop Model VAB 8-14 by Henriksen.

- Polypropylene (melting temp = 130 °C, heat capacity 1920 J/kg °C)
- 15 m long
- 900 kg mass = 8 mops or 112 kg/mop
- Collection yield = 80m^3/h or 10m^3/h per mop (unknown linear rate of the mop)

BLUF: The findings contained here suggest that the surface area of the mop will ultimately determine the heating and cooling rate of the mop. To provide a firm assessment of the heating needs and requirements we must determine the surface are of the rope mop before and after oil recovery from the rope mop and the surface area of the mop in both the wet and dry state. Based on preliminary assessments of the assumed surface area of the mop, heating with steam is the only viable option to prevent icing of the mop. Off-the-shelf steam cleaners/deicers can be obtained for ~$6000.00. In operational settings source for the steam can come from the ship's power plant.

The total surface area for each mop is not given and is therefore "assumed" for this assessment. There are two ways that the surface area was estimated for this assessment.

- Given a collection rate 10 m^3/h per mop, and assuming a mop speed of 1 m/min yields a collection of 0.16 m^3/min or 0.16 m^2/meter length of mop. At 15 m this becomes 2.4 m^2 for the entire mop.
- Alternatively, assuming 2 mm (0.002 m) thickness of oil coating the mop fibers per collection, then 10 m^3/h per mop becomes 5000 m^2/h, or 333 m^2/h or 5.5 m^2/meter length of mop.

With these two extremes we can create a bracket of the expected temperature of the mop for a given condition.

To determine the temperature and heat loss of the rope mop, we must consider the loss of heat to the air due to convection.

The convective heat transfer equation for an object in air is:

$$q_{Air} = (h_{Air} \cdot A \cdot [T_{sK} - T_{AK}]) \cdot t \qquad (1)$$

Where:

$q_{Air} = The\ amount\ of\ heat\ in\ Joules\ lost\ to\ the\ air$

$T_{sK} = Temperature\ of\ the\ surface/object\ (K)$

$T_{AK} = Temperature\ of\ the\ Air\ (K)$

$t = time\ in\ seconds$

$A = Surface\ Area\ of\ the\ object\ (m^2)$

$h_{Air} = The\ convective\ heat\ transfer\ coefficeint\ for\ air\ \left(\frac{W}{m^2 \cdot K}\right)$ Described as:

$$h_{Air} = 10.45 - v + 10v^{\frac{1}{2}}$$

$V = Velocity\ of\ the\ air\ over\ the\ object$

Once we understand how heat is lost to the air during the operation of the mop, the next consideration is how that heat loss affects the temperature of the mop itself:

$$q_{pp} = C_{PP} \cdot m \cdot [T_{iK} - T_{fK}] \qquad (2)$$

Where

$C_{PP} = Heat\ Capcity\ of\ the\ mop\ \left(\frac{J}{kg \cdot K}\right)$ (1920 $\left(\frac{J}{kg \cdot K}\right)$ for polypropylene)

$q_{PP} = The\ amount\ of\ heat\ transfered\ in\ Joules$

$m = mass\ of\ the\ mop\ (kg)$

$T_{iK} = The\ inital\ Temperature\ (K)$

$T_{iK} = The\ final\ Temperature\ (K)$

In the case of using the heat mop in the artic, the initial temperature T_{sK} or T_{iK} of the mop is 0-1 °C as it emerges from the water, and the time 't' is a function of the speed of the mop and the length of the mop from the water to the mop carriage. In an outdoor environment not only does the speed of the mop V_m become important in calculating the convective heat transfer in air but so too does the wind speed V_A.

Thus the heat loss equation for a Foxtail Rope mop becomes:

$$T_m = T_s - \left\{ \frac{\left(\left[10.45 - (V_m + V_A) + 10\sqrt{V_m + V_A}\right] \cdot A \cdot [T_{sK} - T_{AK}]\right) \cdot \left(\frac{d}{V_m}\right)}{C_{PP} \cdot \frac{m}{2}} \right\} \qquad (3)$$

$T_m = Temperature\ of\ the\ mop$ (℃)

$T_s = Temperature\ at\ the\ surface\ of\ the\ water\ or\ strating\ temperature\ of\ the\ mop$ (℃)

$T_{sK} = Temperature\ at\ the\ surface\ or\ strating\ temperature\ (K)$

$T_{AK} = Temperature\ of\ the\ Air\ (K)$

$V_A = Velocity\ of\ the\ Air\ ({}^{m}/_{s})$

$V_m = Velocity\ of\ the\ mop\ ({}^{m}/_{s})$

$A = Surface\ Area\ of\ the\ mop\ (m^2)$

$d = Length\ of\ mop\ out\ of\ the\ water\ (m)$

$C_{pp} = Heat\ Capcity\ of\ the\ mop\ \left(\frac{J}{kg \cdot K}\right)$

The resulting temperature of the mop from this equation becomes the temperature of the mop at the carriage, and takes into account the temperature of the air, the temperature of the water, the speed of the mop, the surface area of the mop, the length of the mop, and the speed of the wind.

To determine the temperature of the mop just before it enters the water, replace the values of T_s and T_{sK} with the temperature that the mop has at the carriage or increase the distance that the mop travels and remove the ½ coefficient from the mass of the mop. This will account for the whole mop moving from the water to the carriage and back to the water.

In a static state, the wind speed can be ignored, and under a constant velocity for the movement of the mop (in this case 1 ft/s or 18 m/min) the convective heat transfer coefficient becomes 15.63 W/m^2K. In which case the temperature of the mop at a given distance or time out of the water can be plotted in terms of temperature versus time/ft-from-the-surface-of-the-water.

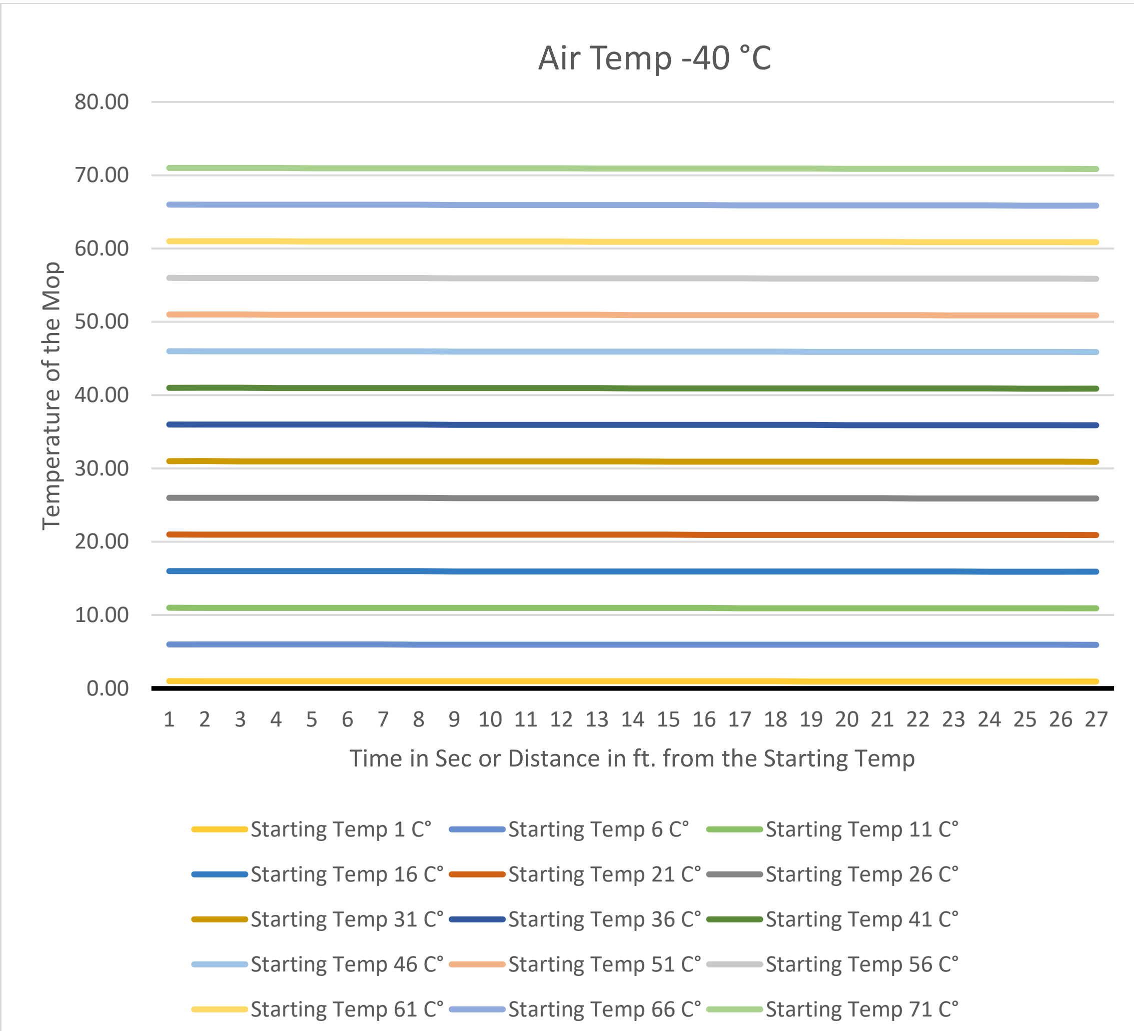

Figure 7: Temp vs. Time of mop at -40 C, with a surface area of 0.16 m²/meter-length of mop.

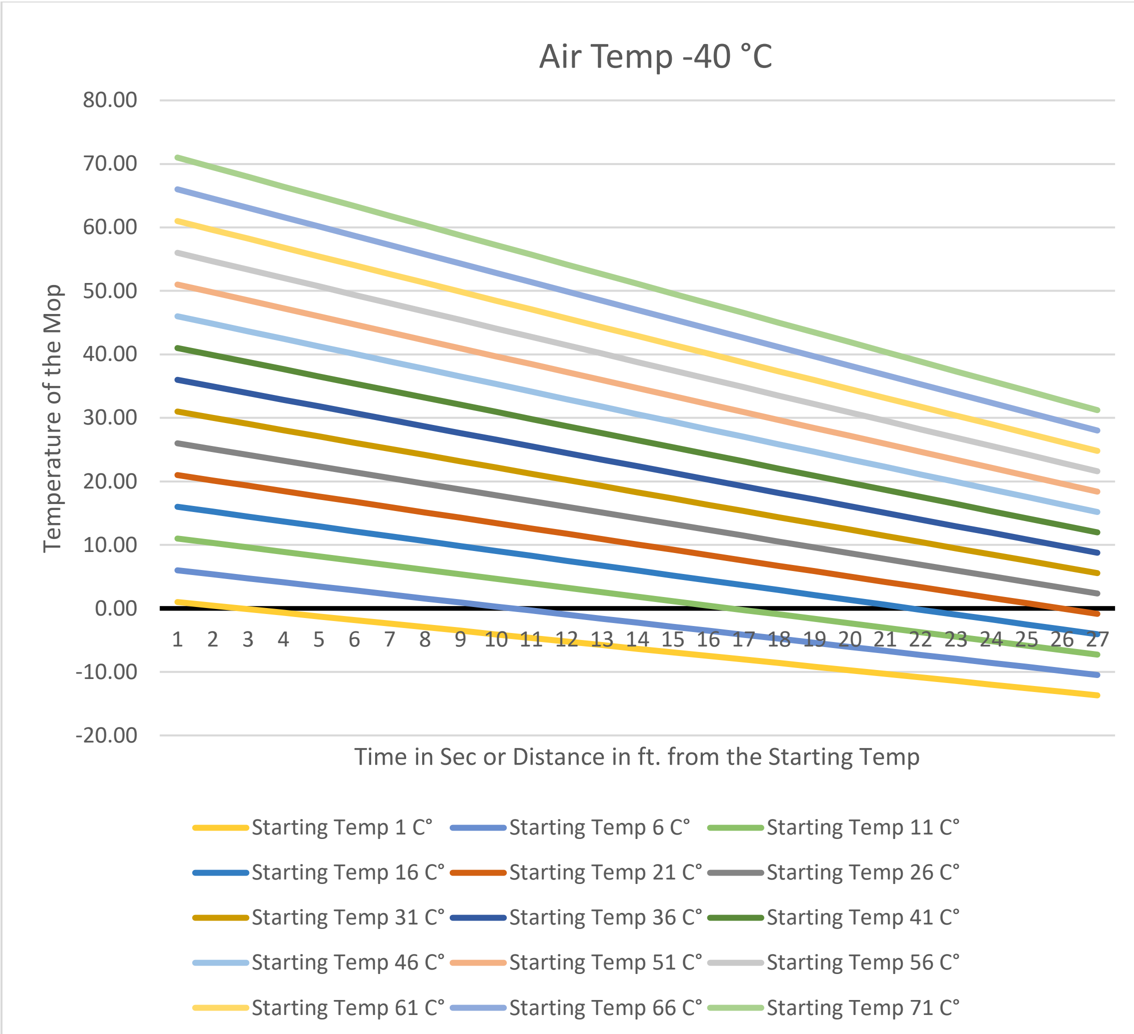

Figure 8: Temp vs. Time of mop at -40 C, with a surface area of 5.55 m²/meter-length of mop.

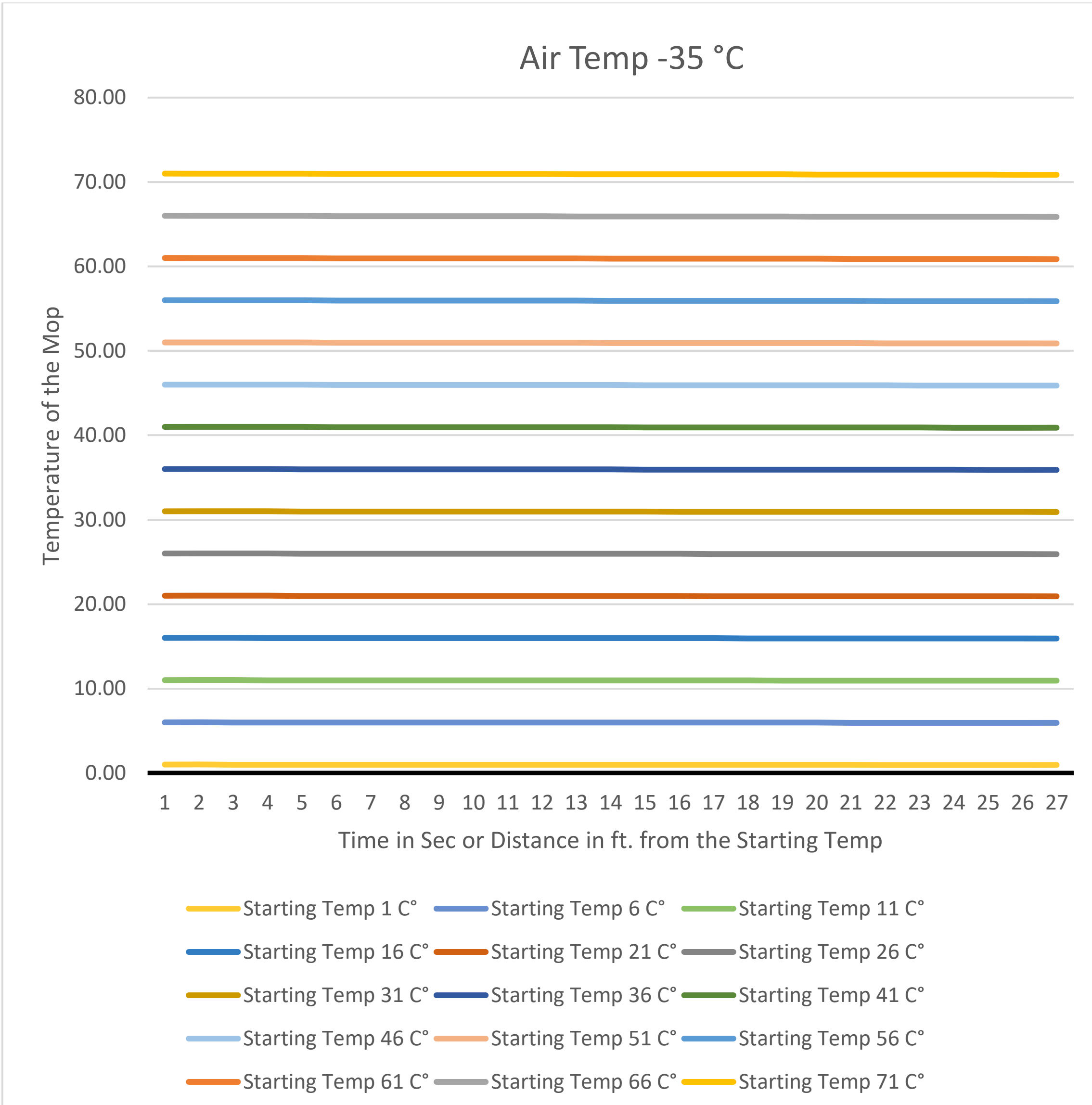

Figure 9: Temp vs. Time of mop at -35 C, with a surface area of 0.16 m²/meter-length of mop.

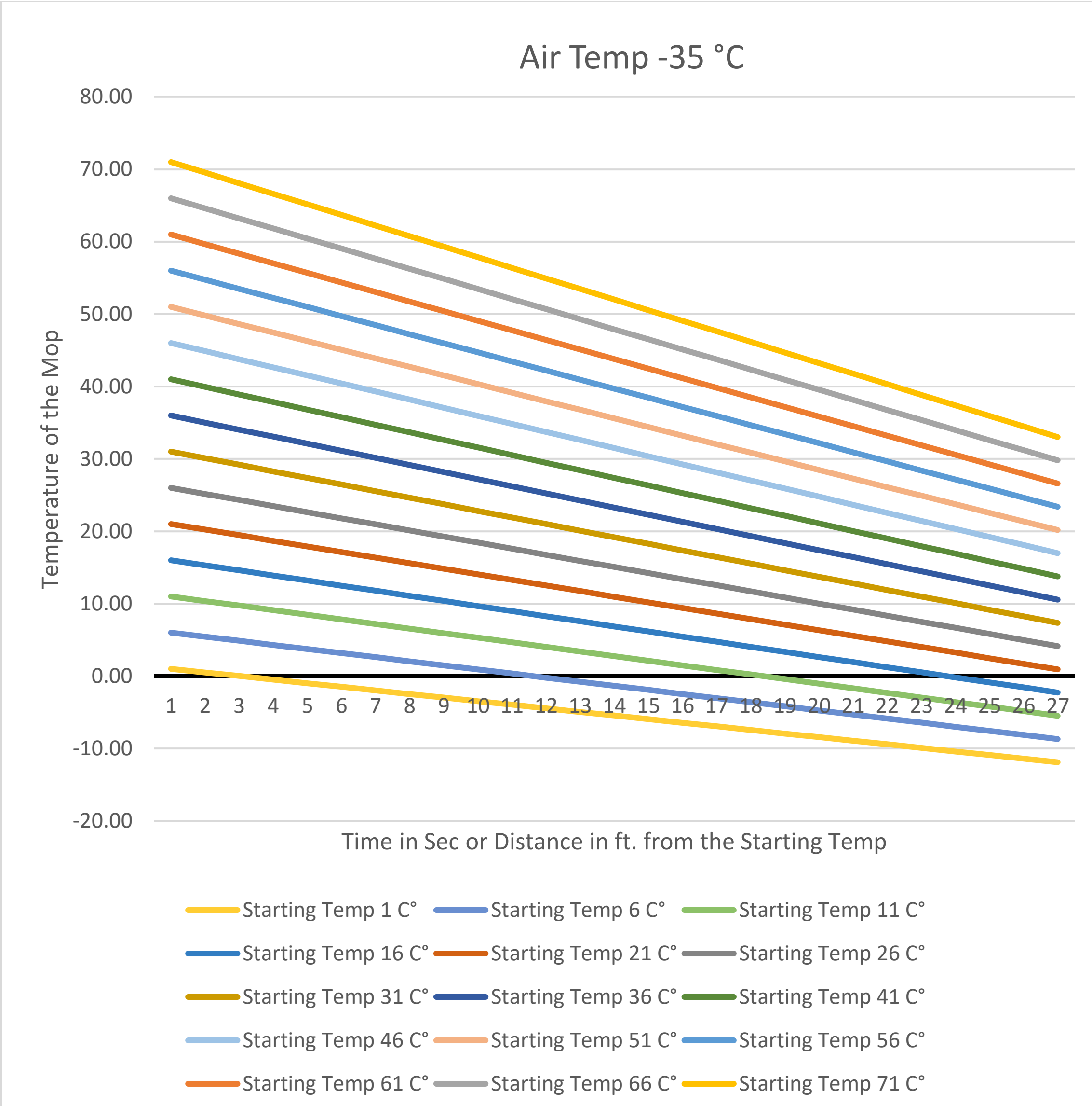

Figure 10: Temp vs. Time of mop at -35 C, with a surface area of 5.55 m^2/meter-length of mop.

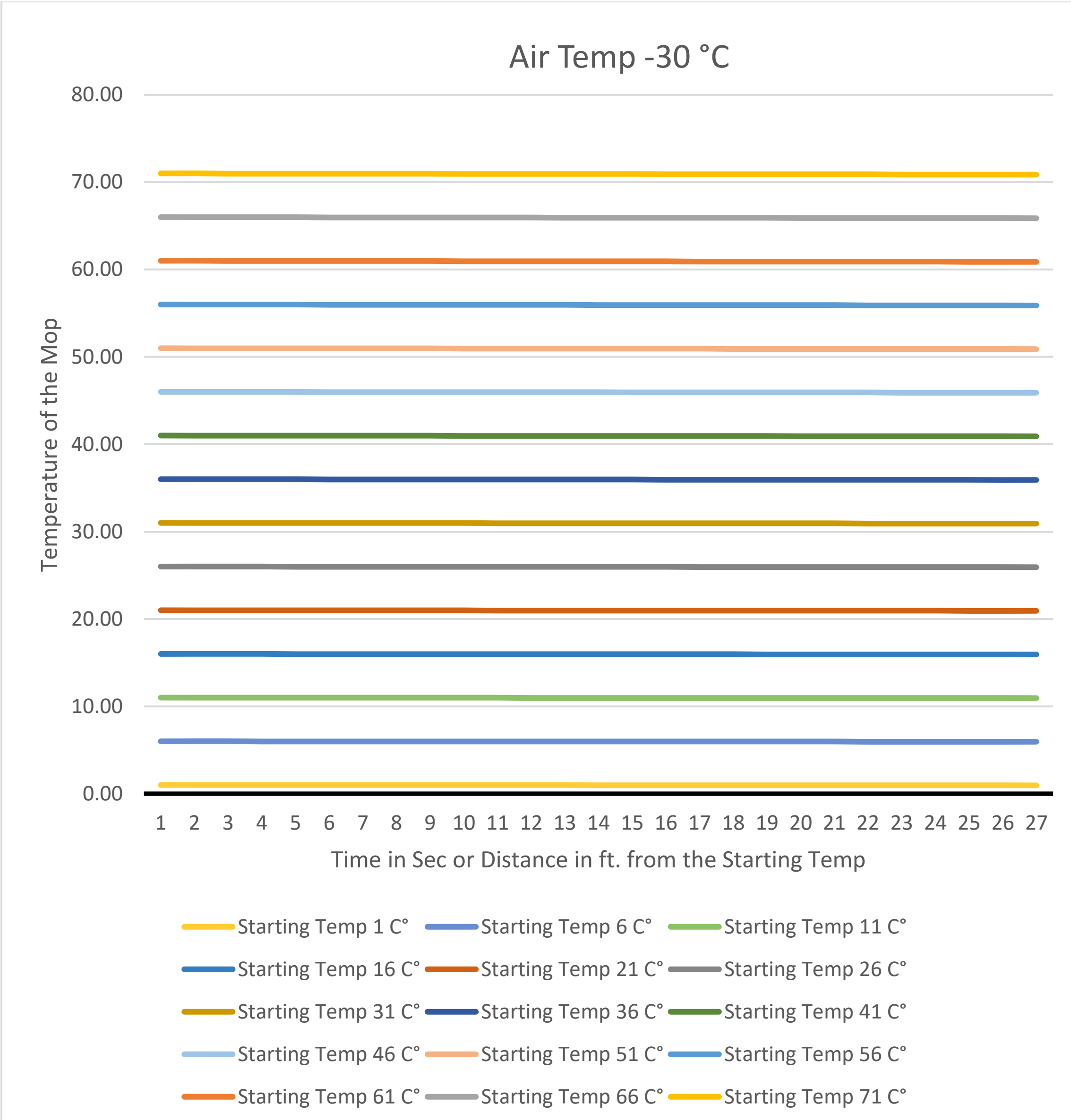

Figure 11: Temp vs. Time of mop at -30 C, with a surface area of 0.16 m^2/meter-length of mop.

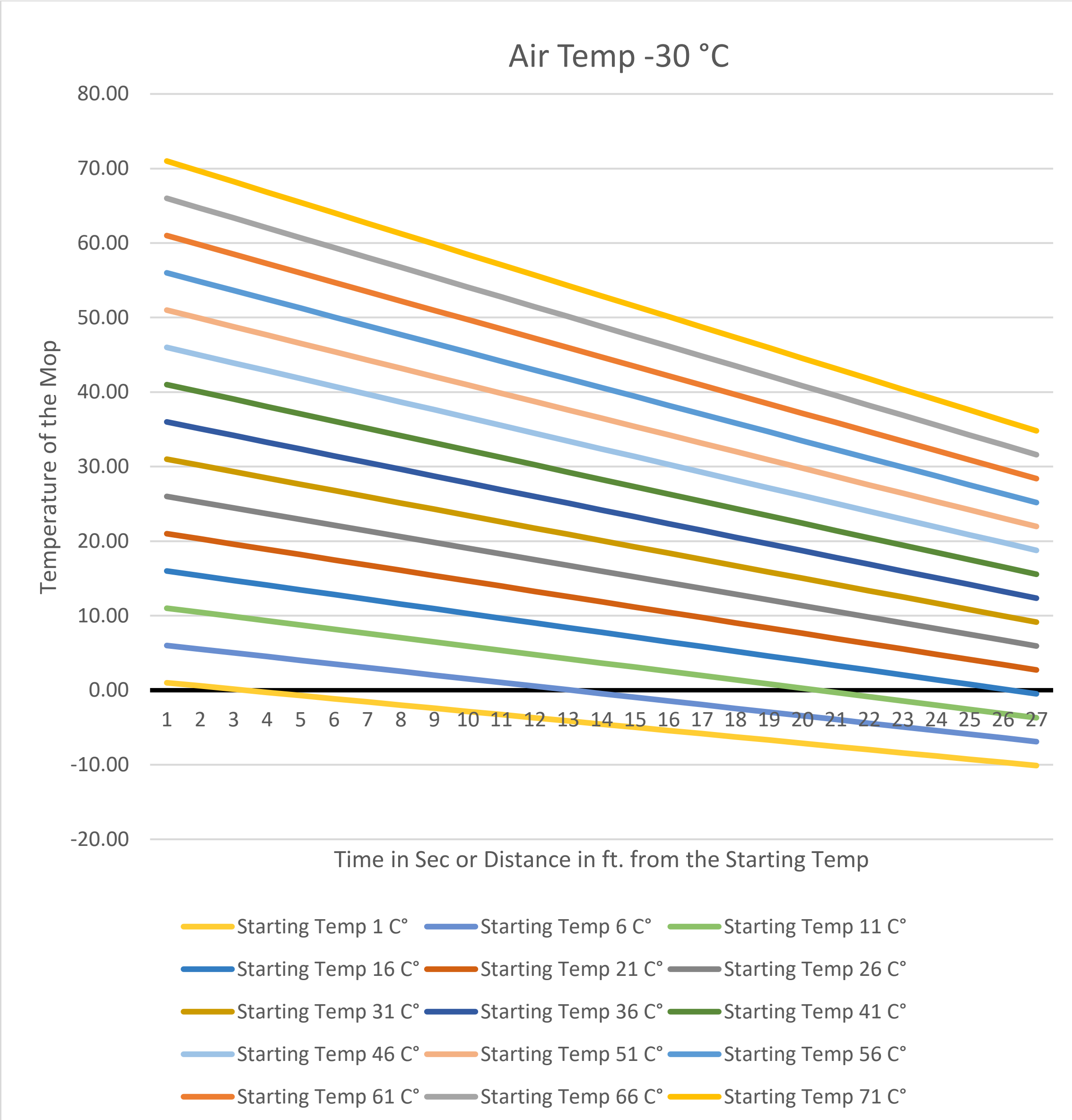

Figure 12: Temp vs. Time of mop at -30 C, with a surface area of 5.55 m^2/meter-length of mop.

As can be seen from the above plots the cooling time and end temperature are greatly dependent on the surface area of the mop, so a true measure of this surface area or a more-true estimate would be needed to provide more realistic values for these cooling rates.

The wind in the arctic region can vary greatly. But there are set guidelines for working in artic environments due to the physical hazards of wind chill. Below is the OSHA recognized Work/Warm-up Schedule for a 4 hour shift in below -26 °C conditions. This matrix gives us an estimate from which to work to determine the cooling rate of the mop in an operational setting.

Work/Warm-up Schedule for a 4-Hour Shift

Air Temperature--Sunny Sky		No Noticeable Wind		5 mph Wind		10 mph Wind		15 mph Wind		20 mph Wind	
°C (approximate)	°F (approximate)	Maximum Work Period	Number of Breaks	Maximum Work Period	Number of Breaks	Maximum Work Period	Number of Breaks	Maximum Work Period	Number of Breaks	Maximum Work Period	Number of Breaks
-26 to -28	-15 to -19	(Normal Breaks) 1		(Normal Breaks) 1		75 min	2	55 min	3	40 min	4
-29 to -31	-20 to -24	(Normal Breaks) 1		75 min	2	55 min	3	40 min	4	30 min	5
-32 to -34	-25 to -29	75 min	2	55 min	3	40 min	4	30 min	5	Non-emergency work should cease	
-35 to -37	-30 to -34	55 min	3	40 min	4	30 min	5	Non-emergency work should cease			
-38 to -39	-35 to -39	40 min	4	30 min	5	Non-emergency work should cease					
-40 to -42	-40 to -44	30 min	5	Non-emergency work should cease							
-43 & below	-45 & below	Non-emergency work should cease									

Schedule applies to any 4-hour work period with moderate to heavy work activity; with warm-up periods of ten (10) minutes in a warm location and with an extended break (e.g. lunch) at the end of the 4-hour work period in a warm location.

Adapted from ACGIH 2012 TLVs

Image 1: *https://www.osha.gov/dts/weather/winter_weather/windchill.html*

As can be seen in the above schedule no work is conducted when the outside temperature is less than -43 °C and the there is a noticeable wind. So no considerations were made for wind chill at -40 °C. Given that the "wind chill" in each these conditions is essentially unchanging with increases in temperature and wind speed, the considerations of heat lost with wind were only considered for the worst case -35 °C at a wind speed of 8 km/hr and compared to a static condition of both -35 °C and -40 °C with no wind.

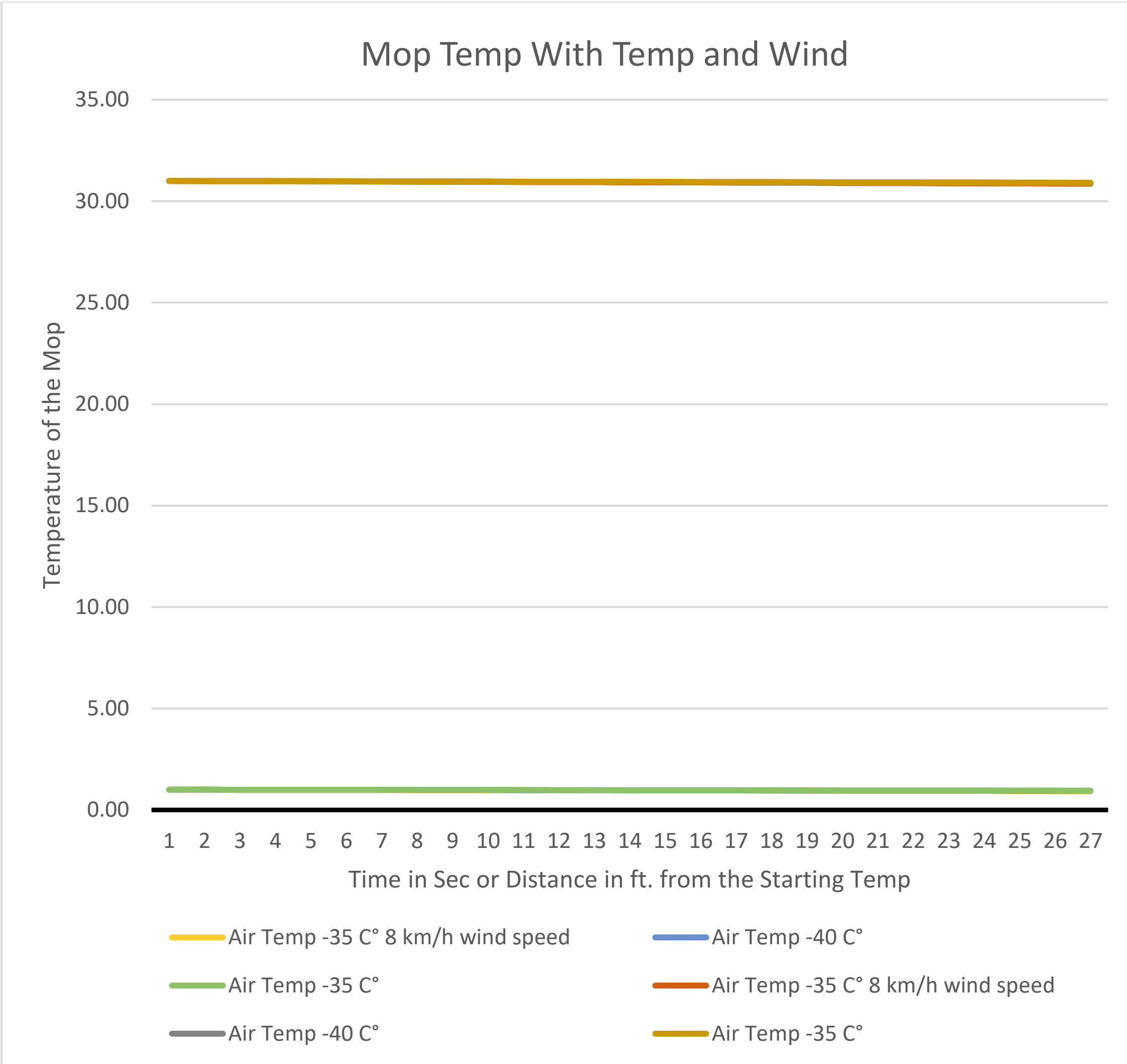

Figure 7: Temp vs. Time of mop at various temperatures and wind speeds, with a mop surface area of 0.16 m^2/meter-length of mop.

As can be seen in the plot above, for a mop with a surface area of 0.16 m^2/meter-length of mop regardless of the temperature or wind speed the final temperature will not change significantly from the starting temperature. This data suggests that no significant heating is required for mops of this surface area.

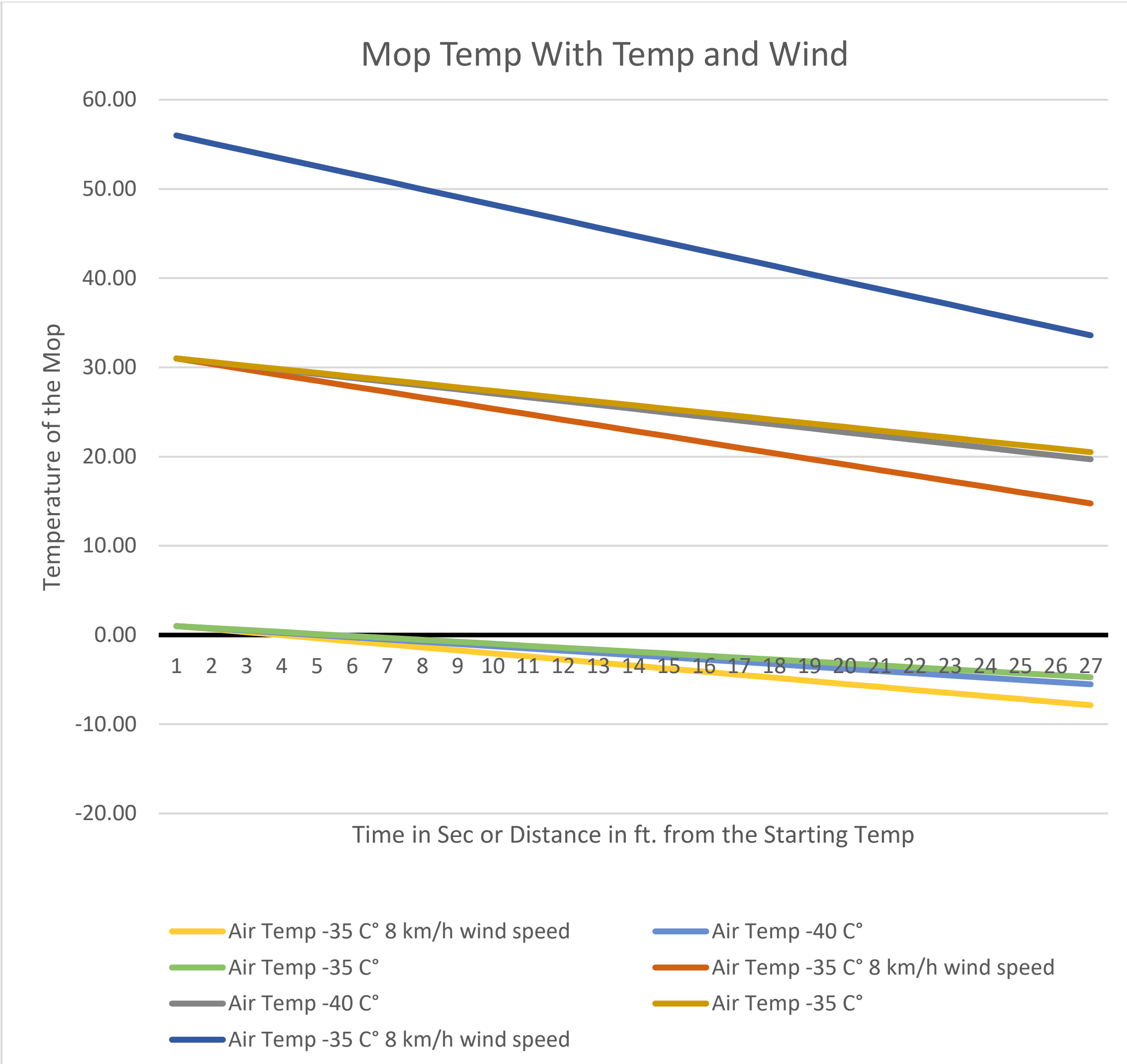

Figure 8: Temp vs. Time of mop at various temperatures and wind speeds, with a mop surface area of 5.55 m^2/meter-length of mop.

As can be seen in the plot above, for a mop with a surface area of 5.55 m^2/meter-length of mop, there will be a significant drop in temperature with respect to the initial temperature of the mop. This data suggests that for mops with this much surface area, a heating to temperatures of 30-40 °C will be required to prevent the formation of ice.

Energy Required to Heat a Rope Mop to Prevent Icing

Assuming the worst case scenario above, using a rope mope with a surface area of 5.55 m^2/meter-length and an outdoor temperature of -35° C with a wind speed of 8 km/hr, the ΔT required to make sure the mop does not reach a freezing temperature is ~50° C. Assuming the worst case surface area, and an air temperature of -40 C° with no wind, then the ΔT required for the mop is only ~30° C. Using these two limits we can determine how much energy per unit time is required to heat the mop to these temperatures.

Polypropylene has a heat capacity of 1920 $\left(\frac{J}{kg\cdot K}\right)$ and each 15 m length of mop has a mass of 112 kg, or 7.46 kg/meter-length, using Eqn. 2 a ΔT = 40° C needs 572,928 Joules (573 kJ) per meter of mop. Assuming that only 1 meter of mop can be heated at a time, and the mop is moving at 18 m/min, this allows for 3 seconds of heating per meter of mop or 190,976 Watts (191 kW) of power. *Even ignoring the need to heat the air around the mop, a direct heating of the mop at 191 kW is not practical using IR heaters or heating mats.* The mop is moving too fast and requires too much heat (due to the heat capacity). With a ΔT = 30°, the heating requirements drop to 142.8 kW of power, which is still not practical.

Forced Air Heating

When we consider forced air propane heaters, a low end unit may produce 35,000 BTU/hr and a high end heater may produce 135,000 BTU/hr. This translates to 10.25 kW and 39.6 kW respectively. These wattages will provide a change of 2.1° C and 8.3° C respectively assuming that the surrounding air does not have to be heated. If the mop has a temperature of -8° C by the time it reaches the heat source then this heating will not be enough to prevent freezing or melt any ice being collected. If the oil protects the mop such that by the time it reaches the carriage and while it is being cleaned, then if the mop has a starting temperature of 1° C prior to heating, at -40° C with no wind, the mop will reach freezing temperatures within 3 to 15 seconds <u>after</u> being heated (or 10-22 ft. before it enters the water). Thus for this scenario the direct heating of the mop using forced air propane heaters is not practical.

Image 2: http://www.homedepot.com

Steam Heating

Polypropylene has a melting temperature of 130° C. Given this tolerance it may be possible to use steam as a direct heating source for the mop.

In contrast to convection, heat transfer via condensation from steam is continuous. As the steam condenses on the surface, the latent heat of the steam is transferred to the material, but the steam condensate on the surface of the material is also maintained at the same temperature of the steam that produced it. In other systems where heat is transferred via convention the temperature of the heat source changes as heat is lost to the receiving material, leading to uneven heating and larger heat requirements from the source. With steam heating the amount of latent heat released is 2 to 5 times greater than the amount of sensible heat available from a fluid such as hot water.

The latent heat of condensation from steam is 2264.76 J per gram of water. With a required heat load of 716,160 Joules, 317 mL (6.34 L/min) of steam is required to raise the temperature of 1 meter of mop by 50° C. With a surface area of 5.55 m^2, 317 mL will cover 1 meter of mop with a layer only 0.005 mm thick.

Image 3: http://www.sioux.com/thawing-de-icing-systems-applications.html

The heat capacity of water is 4182 J/kgC. At an air temperature of -35° C and a wind speed of 8 km/hr, the condensed water covering a 1 meter length of mop at this thickness, with a mass of 0.317 kg, and a starting temperature of 100° C, will reach freezing temperatures within 8 seconds, or 8 ft after leaving the point of being heated by the steam nozzle. This assessment was determined by modifying equation 3, with the values for water on the surface of the mop. See Below.

$$T_{m_{Water}} = T_s - \left\{ \frac{\left([10.45-(V_m+V_A)+10\sqrt{V_m+V_A}]\cdot A\cdot[T_{sK}-T_{AK}]\right)\cdot\left(\frac{d}{V_m}\right)}{c_{PP}\cdot m} \right\} \qquad (4)$$

$T_m = Temperature\ of\ the\ mop\ (°C)$

$T_s = Strating\ temperature\ of\ the\ water\ costing\ the\ mop\ (°C)$

$T_{sK} = Temperature\ at\ the\ surface\ or\ strating\ temperature\ (K)$

$T_{AK} = Temperature\ of\ the\ Air\ (K)$

$V_A = Velocity\ of\ the\ Air\ (^m/_s)$

$V_m = Velocity\ of\ the\ mop\ (^m/_s)$

$A = Surface\ Area\ of\ the\ mop\ (m^2)$

$d = Length\ of\ mop\ covered\ in\ water\ (m)$

$C_{pp} = Heat\ Capcity\ of\ the\ mop\ \left(\frac{J}{kg\cdot K}\right)$

With these considerations, steam can be used to heat the mop more efficiently than force air or IR heaters, but the added water that coats the mop will freeze before the mop reaches the surface of the ocean. In this scenario it would make sense to position the steam nozzle close to where the mop enters the ocean, but such positioning of the nozzle so close to the surface of the water could disrupt and scatter the oil that the mop is trying to collect.

As in earlier calculations of heat loss from the mop, the heat loss of the water that is coating the mop is dependent on the surface area of that coating. In the plot shown below, the temperature change over time with and without wind, was made assuming a surface area of 5.55 m^2/meter-length of mop. As the above calculations show, this layer of water is too thin to maintain any sort of temperature. If the water does not vaporize immediately after condensing on the mop it will likely form ice crystals on the surface of the mop before this 8 second time period has even lapsed.

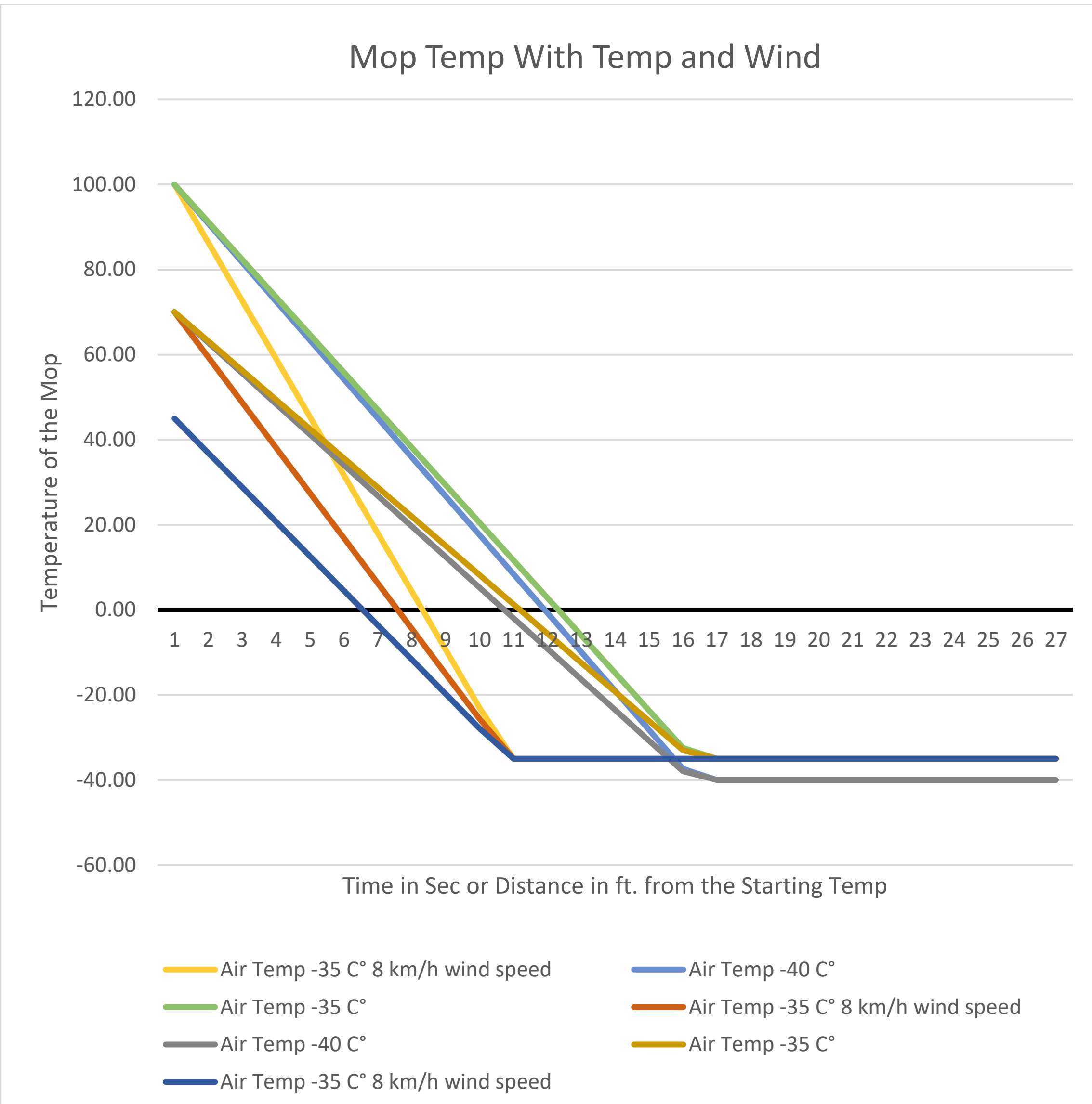

Figure 9: Temp vs. Time of water on the surface of mop at various temperatures and wind speeds, with a mop surface area of 5.55 m^2/meter-length of mop.

The above plot assumes that the water condensate on the mop is coating every surface of every bristle of the mop for that 1 meter length. But this is an unlikely case given both the surface tension and cohesive nature of water. The water will most likely spread across several bristles and not fully encase each bristle individually. With a 14" (0.35 m) wide mop, and assuming that the bristles are 1 mm thick, if the water collectively coats all the bristles and effectively creates a two sided 0.35 x 1 meter blade per meter length of mop, the surface area of the water coating will be ~0.7 m^2. This translates into a layer of water 4.5 mm thick coating the mop blade.

The plot below demonstrates that this low surface area and thick water shell is enough to maintain the temperature of the mop in the worst conditions (the air temperature is -35° C with a wind speed of 8 km/hr) even if the starting temperature of the condensed water coating the mop is only 45° C; a little less than the 50° C temperature that the mop had been heated to using the steam.

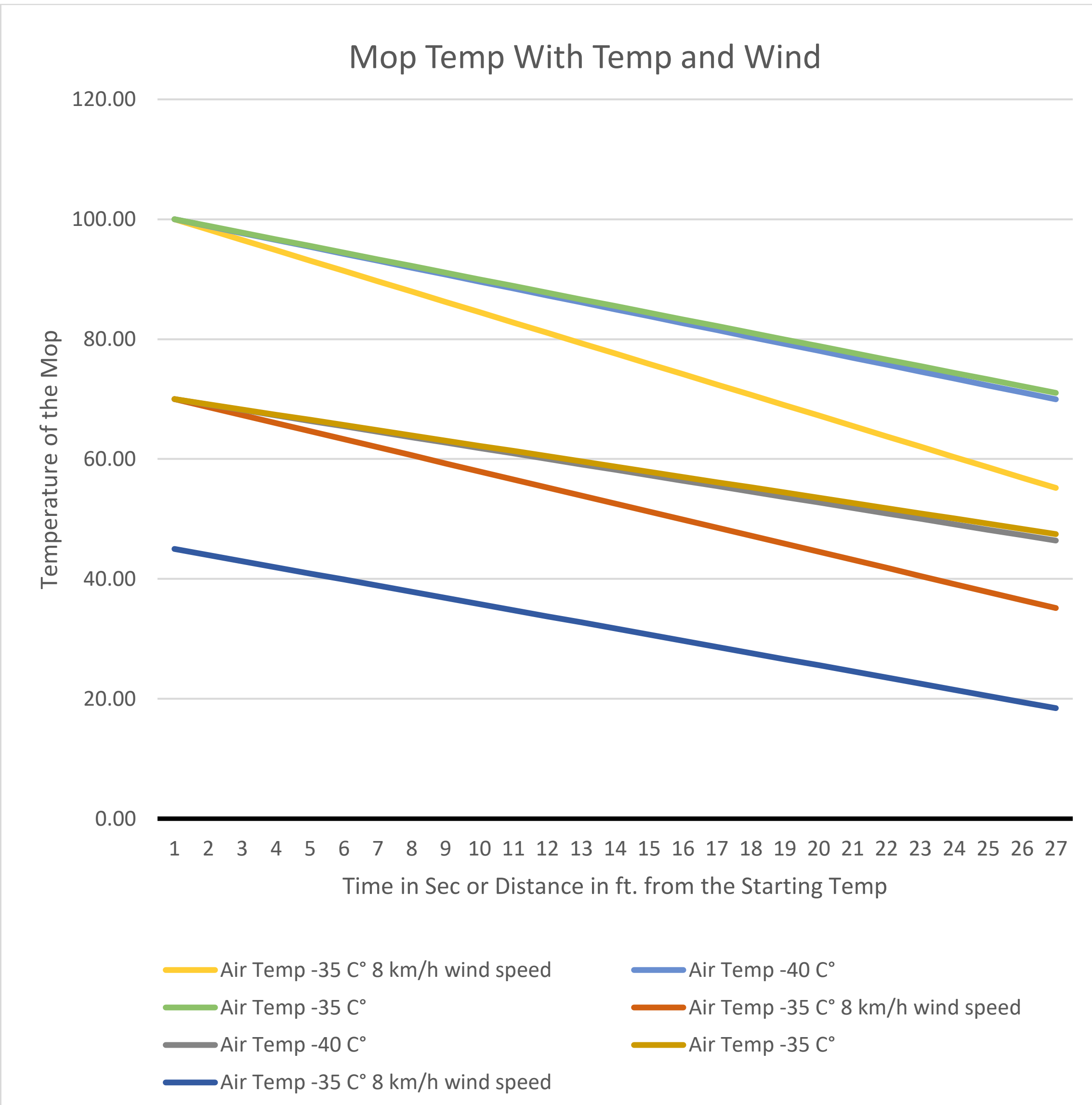

Figure 10: Temp vs. Time of water on the surface of mop at various temperatures and wind speeds, with a mop surface area of 0.7 m^2/meter-length of mop.

The above plot shows that steam heating would be the ideal solution to heating the mop if and only if the water coating the mop creates a shell that significantly reduces the surface area to below 1.1 m^2/meter-length of mop. Under these conditions the 3 second heating per 1 meter length of mop using steam can be done at the mop carriage, after the oil had been collected, such that the steam jet will not disrupt the oil that the mop is collecting on the surface of the water. Steam can be generated using simple gas/electric powered steam/cleaners/washers/deicers and can be obtained for as little as ~$6000.00. The steam could also be generated from the cooling system attached to the power plant of the coast guard cutter that is using the mop.

Inverting the Solution

Since the icing and gumming of the skimmer mop due to low temperature ultimately adversely affects the mop carriage and oil collection system, an inversion to the problem is not to heat/deice the mop, but rather heat and deice the carriage. Heating the carriage will prevent gumming and ice buildup at the location where it is of most concern. The heating of the carriage will by extension heat the mop and minimize future operational fouling. The carriage can be heated continuously using heat mats attached to the shell and even internal piping of a steam with the condensate being piped back to the steam source or ship. The carriage is metallic and therefore the thermal conductivity will allow the heating to spread throughout the structure of the carriage. Insulation can be applied to the exterior of the carriage to direct any radiant heat toward the interior and towards the rope mop within the carriage.

Further Considerations of Surface Area

As can be seen in the images below, the rope mop is a fine collection of polypropylene bristles and depending on the age, use, and what the mop is coated with as it skimming, the effective surface area of the mop is always changing. The above calculations were done based on assumptions about the mop as it is picking up oil, but as can be seen in the pictures the mop has the potential for even higher surface areas as it dries or as oil is removed.

Image 3: Courtesy of Henriksen

With a dry mop if we assume that for a 1 meter length the polypropylene is just a flat blade 0.35 m wide and 0.001 m thick, then the surface area is 2 x 0.35 m + 0.001 x 1 m + 2 x 0.35 x 0.001 m (accounting for the three exposed edges of the blade) which comes to 0.7017 m^2.

If there are two side to this mop (divided by the center cable that runs through the mop) it is 0.7017 m^2 across the two sides. If each of the two

Image 4: Courtesy of Henriksen

sides/blades of the mop are cut in half parallel to the shortest edge (perpendicular to the center cable), then two new surfaces are created for each side or now 4 blades that are 0.175 m wide and 0.5 m long, each with 3 edges 1 mm thick, which adds to the above calculation **2 x 0.35 x 0.001 m** + 2 x 0.35 m + 0.001 x 1 m + 2 x 0.35 x 0.001 m = 0.7024 m^2. Another way to see this is the equation below:

$$(2 \cdot Width)(1 + Thickness) + (Length \cdot Thickness) + (2 \cdot Width \cdot Thickness \cdot \# \, of \; Cuts)$$

If the number of cuts or divisions is zero then the surface area is that of the two blades (divided by the center cable). As successive cuts into the blade are made, the number of blades per side of mop is then 2 times the number of cuts (each cuts makes two extra edges). At 500 cuts there are 1000 blades on each side of the mop each 0.001 m long, 0.001 m thick and 0.175 m in width. This makes 2000 bristles per meter length of mop or a surface area of 1.0517 m^2/meter-length of mop.

This value falls between the two surface area examples outlined above, but the question still remains what is the actual surface area of the mop under various working conditions?

Image 5: Courtesy of Henriksen

Image 6: Courtesy of Henriksen

Anticipated Heating Requirements

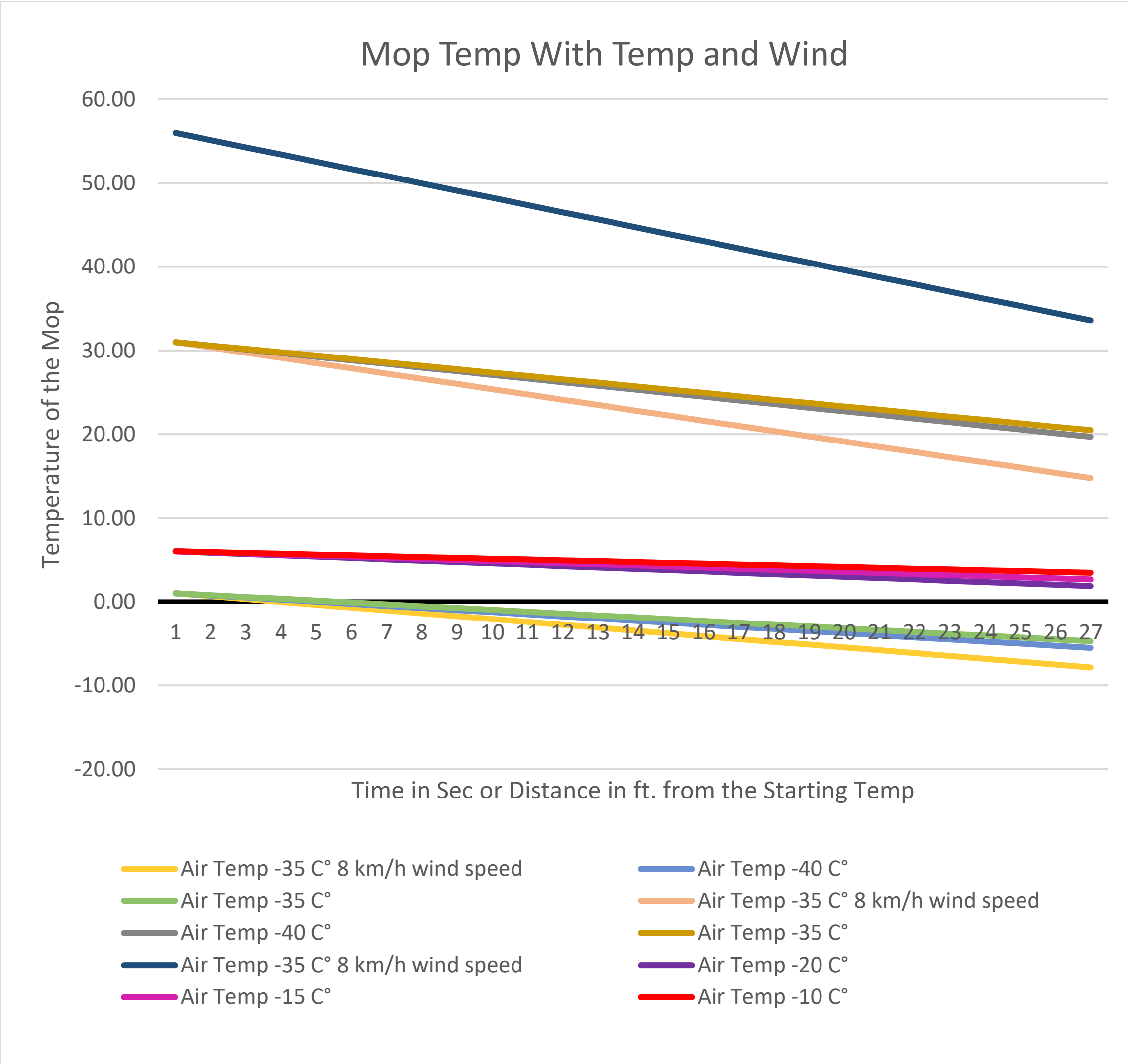

Figure: Temp vs. Time of mop at various temperatures and wind speeds, with a mop surface area of 5.55 m^2/meter-length of mop.

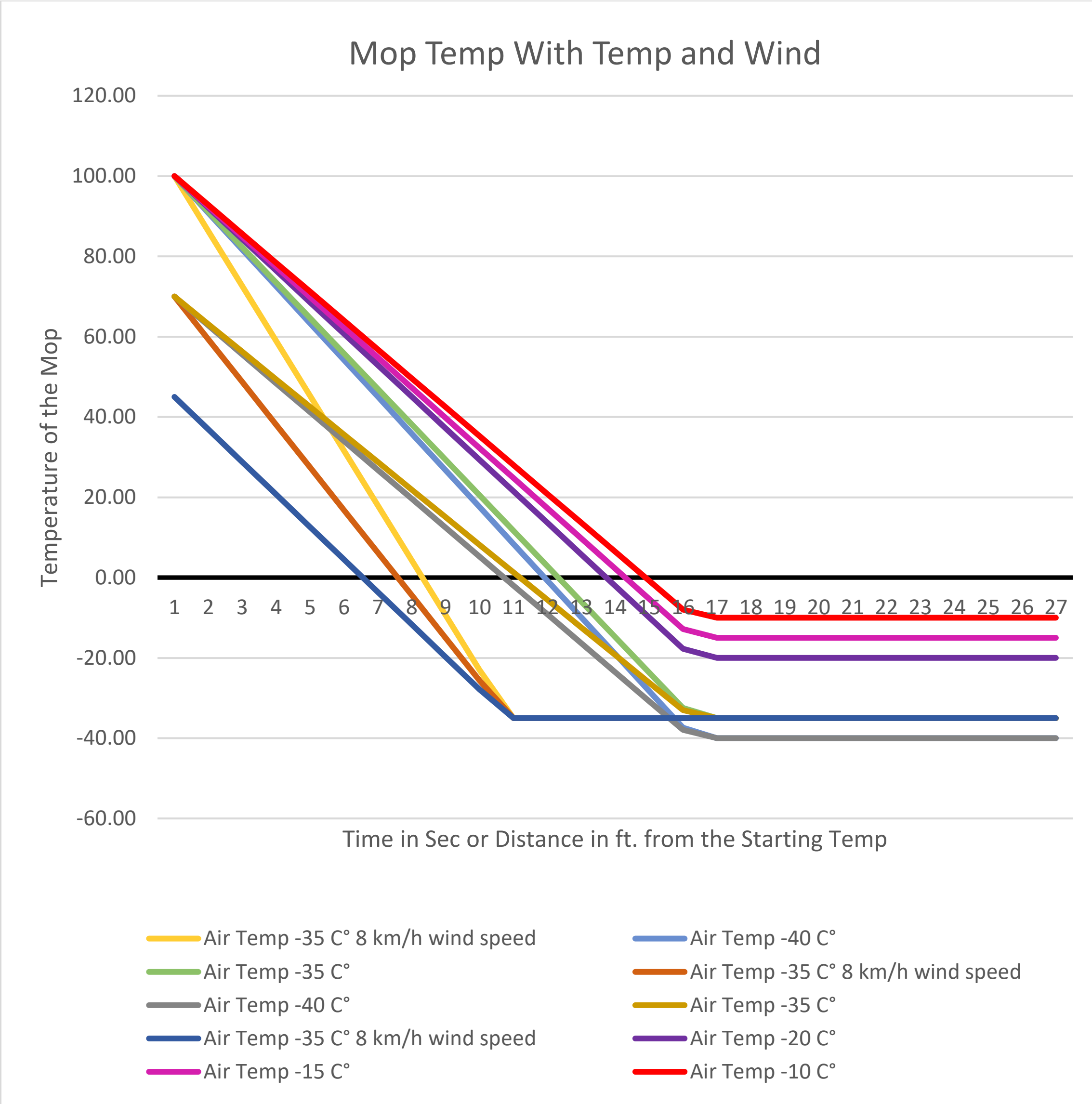

Figure: Temp vs. Time, of water on the surface of mop at various temperatures and wind speeds, with a mop surface area of 5.55 m^2/meter-length of mop.

The above plots show that only a change of 6° C is required to keep the mop from freezing or 30 kW of heat per meter of mop for 3 seconds. Previous calculations suggest that this can be achieved using force-air propane heaters.